Far-infrared spectroscopy of a globule in Cygnus X

Nicola Schneider, Markus Röllig

I. Physik. Institut, University of Cologne,

Germany

SOFIA teletalk 10th november 2021

Introduction

Stellar feedback (radiation, winds) produces various features in the interface region between the molecular cloud and the HII region:

Carina

Hubble

‘Pillars of creation’ in M16

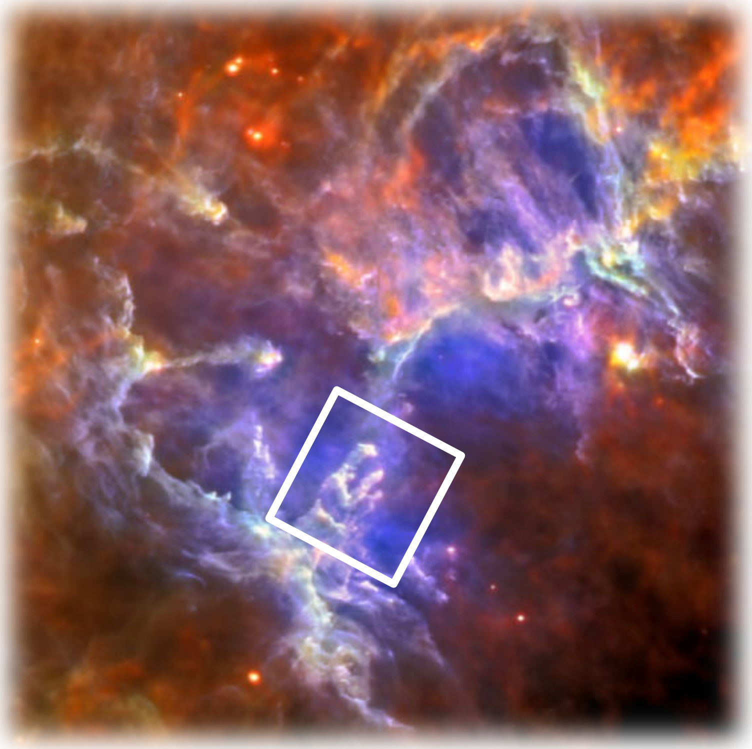

Herschel (HOBYS)

Introduction pillars, globules, EGGs, ...

Not only pillars, a full zoo of features ....

(Schneps et al. 1980; Hester et al. 1996; White et al. 1997; Pound 1998; Pound et al. 2003; Bally & Reipurth 2003;….).

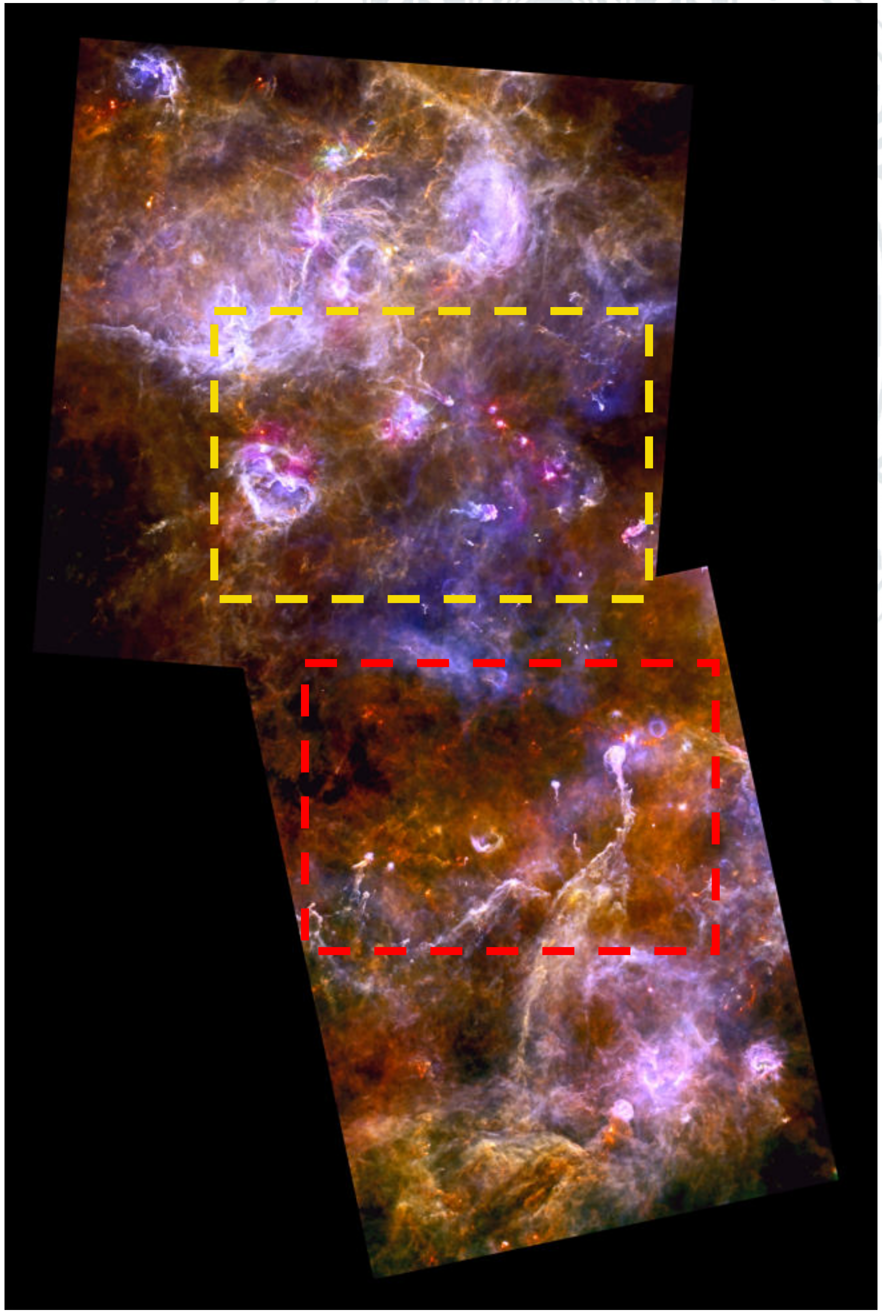

Herschel image (70, 160, 250 µm) of Cygnus X (HOBYS)

Hennemann et al. 2012, Schneider et al. 2016

Pillars column-shaped, attachted to the molecular cloud, ~0.5 to a few pc

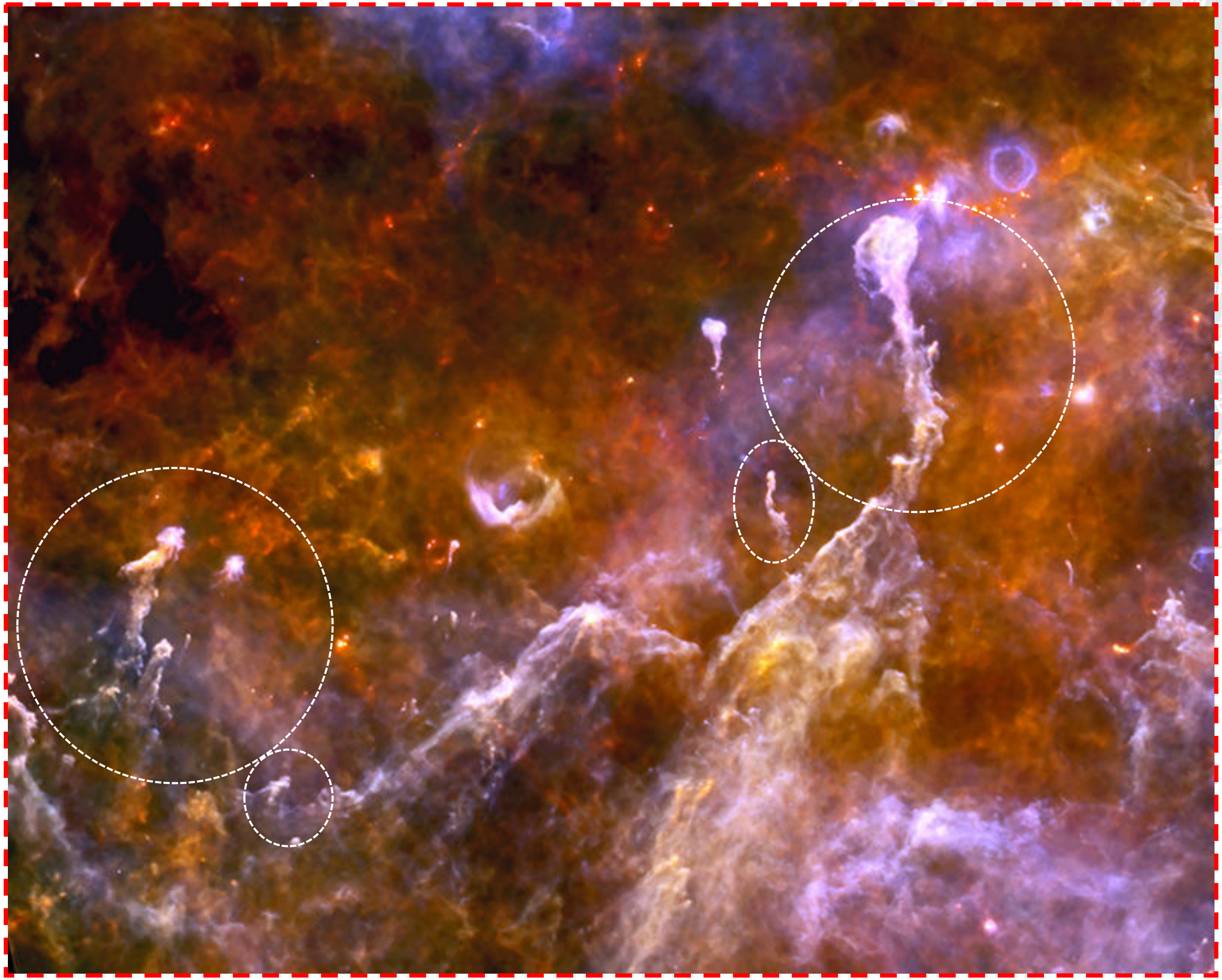

Globules

free-floating, head-tail (tadpole) structure, ~0.5 to a few pc

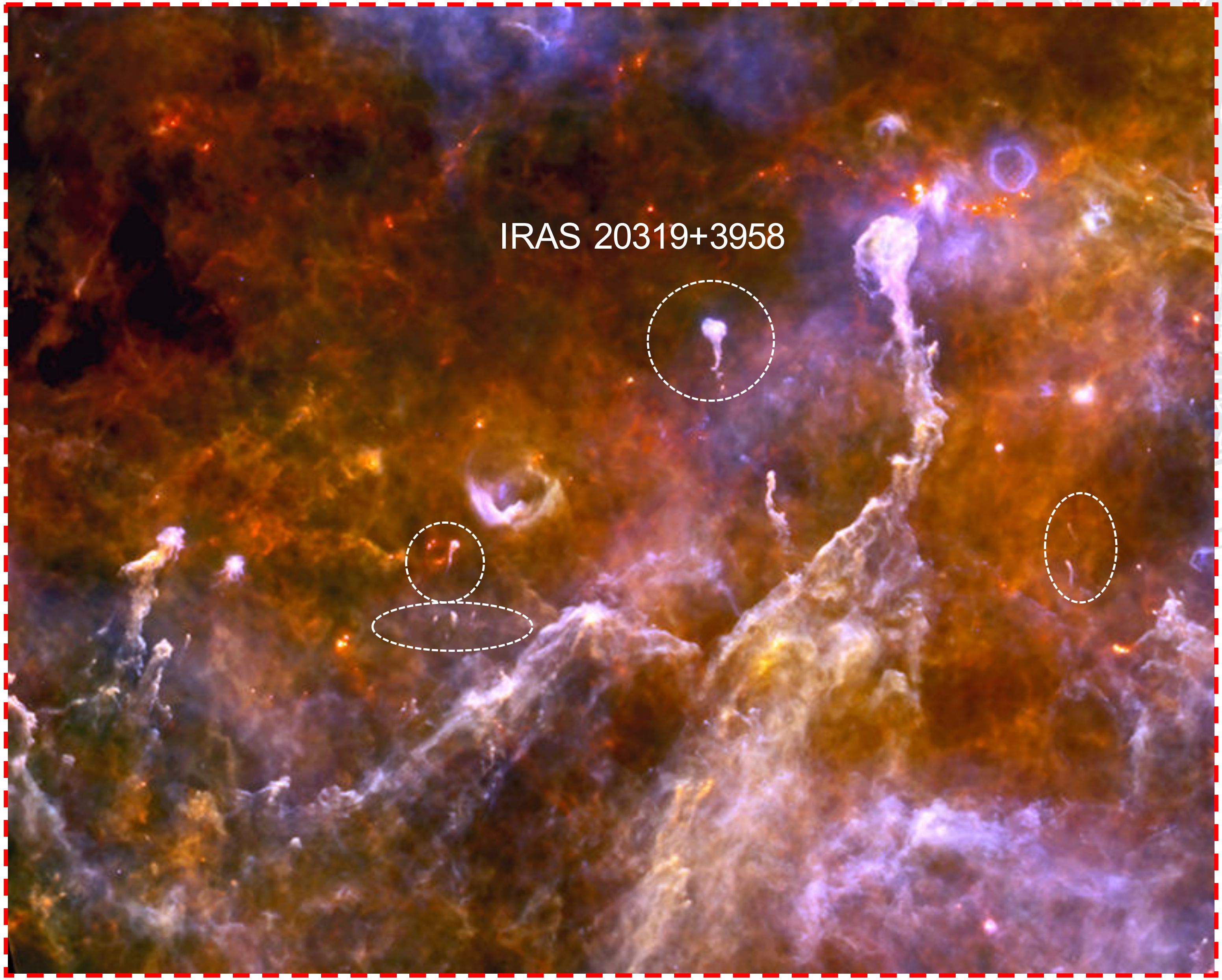

Proplyds evaporating protoplanetary disks

On smaller scales: EGGs (evaporating gaseous globules), teardrop globules, cometary globules, globulettes, ...

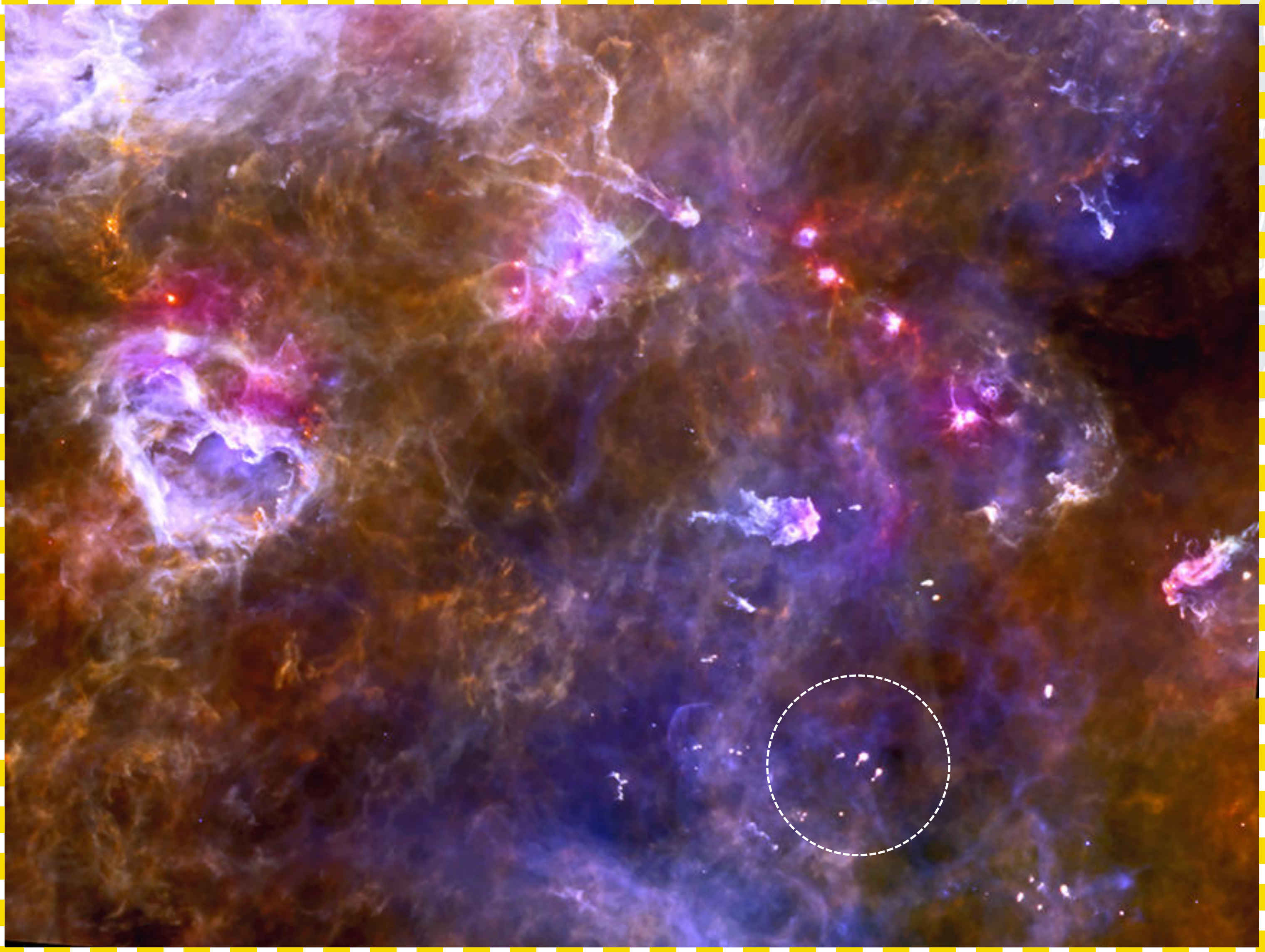

Classification in Cygnus X (Schneider et al. 2016)

- Identification from 70 µm imaging
- Physical properties from dust column density and temperature maps

Globules

- dense $<n> \sim 1.2\ 10^4$ cm^{-3}
- massive $<M> \sim 470$ M$_{sun}$

Pillars

- less dense $<n> \sim 0.5\ 10^4$ cm^{-3}
- massive $<M> \sim 534$ $_{Msun}$

- Pillars and globules have the longest photoevaporation lifetimes (a few 10^6 yr), all other features $<10^6$ yr.
- t_{ff} (free-fall time) a few 10^5 yr

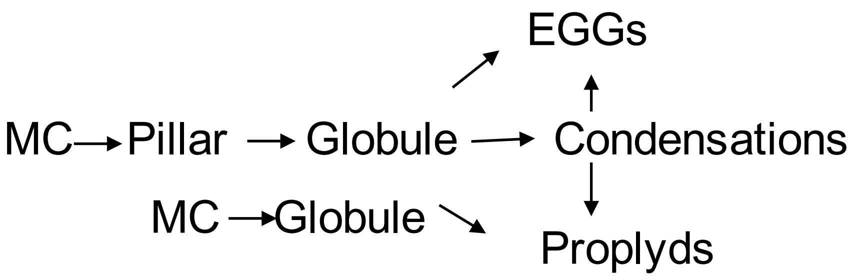

EGGs

MC → Pillar → Globule → Condensations

MC → Globule

Proplyds

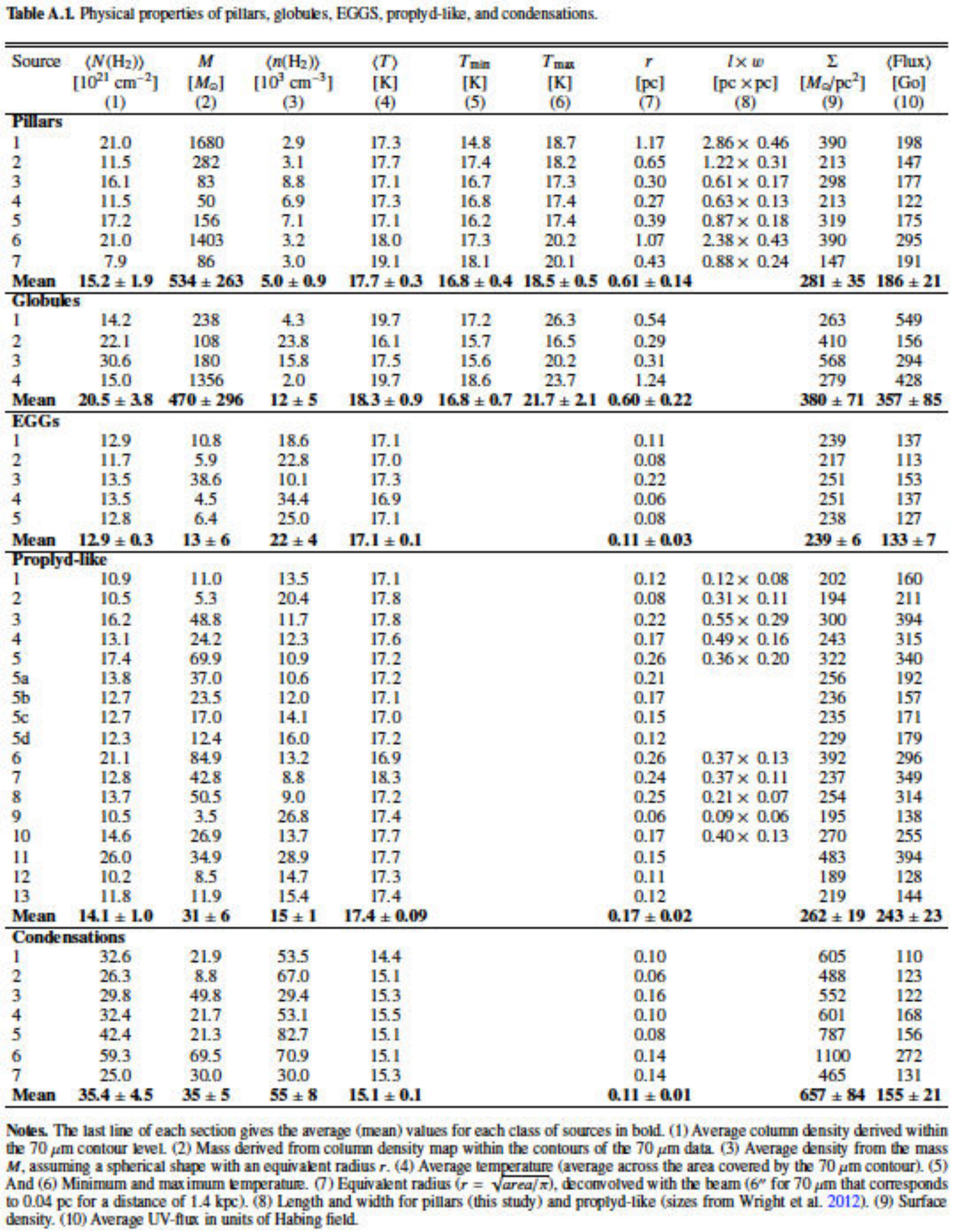

Table A.1. Physical properties of pillars, globules, EGGS, proplyd-like, and condensations.

Source	$\langle N(H_2)\rangle$ [10^{21} cm^{-2}] (1)	M [$M_\odot$] (2)	$\langle n(H_2)\rangle$ [10^3 cm^{-3}] (3)	$\langle T\rangle$ [K] (4)	T_{min} [K] (5)	T_{max} [K] (6)	r [pc] (7)	$l \times w$ [pc × pc] (8)	Σ [$M_\odot$/pc^2] (9)	⟨Flux⟩ [Go] (10)
Pillars										
1	21.0	1680	2.9	17.3	14.8	18.7	1.17	2.86 × 0.46	390	198
2	11.5	282	3.1	17.7	17.4	18.2	0.65	1.22 × 0.31	213	147
3	16.1	83	8.8	17.1	16.7	17.3	0.30	0.61 × 0.17	298	177
4	11.5	50	6.9	17.3	16.8	17.4	0.27	0.63 × 0.13	213	122
5	17.2	156	7.1	17.1	16.2	17.4	0.39	0.87 × 0.18	319	175
6	21.0	1403	3.2	18.0	17.3	20.2	1.07	2.38 × 0.43	390	295
7	7.9	86	3.0	19.1	18.1	20.1	0.43	0.88 × 0.24	147	191
Mean	**15.2 ± 1.9**	**534 ± 263**	**5.0 ± 0.9**	**17.7 ± 0.3**	**16.8 ± 0.4**	**18.5 ± 0.5**	**0.61 ± 0.14**		**281 ± 35**	**186 ± 21**
Globules										
1	14.2	238	4.3	19.7	17.2	26.3	0.54		263	549
2	22.1	108	23.8	16.1	15.7	16.5	0.29		410	156
3	30.6	180	15.8	17.5	15.6	20.2	0.31		568	294
4	15.0	1356	2.0	19.7	18.6	23.7	1.24		279	428
Mean	**20.5 ± 3.8**	**470 ± 296**	**12 ± 5**	**18.3 ± 0.9**	**16.8 ± 0.7**	**21.7 ± 2.1**	**0.60 ± 0.22**		**380 ± 71**	**357 ± 85**
EGGs										
1	12.9	10.8	18.6	17.1			0.11		239	137
2	11.7	5.9	22.8	17.0			0.08		217	113
3	13.5	38.6	10.1	17.3			0.22		251	153
4	13.5	4.5	34.4	16.9			0.06		251	137
5	12.8	6.4	25.0	17.1			0.08		238	127
Mean	**12.9 ± 0.3**	**13 ± 6**	**22 ± 4**	**17.1 ± 0.1**			**0.11 ± 0.03**		**239 ± 6**	**133 ± 7**
Proplyd-like										
1	10.9	11.0	13.5	17.1			0.12	0.12 × 0.08	202	160
2	10.5	5.3	20.4	17.8			0.08	0.31 × 0.11	194	211
3	16.2	48.8	11.7	17.8			0.22	0.55 × 0.29	300	394
4	13.1	24.2	12.3	17.6			0.17	0.49 × 0.16	243	315
5	17.4	69.9	10.9	17.2			0.26	0.36 × 0.20	322	340
5a	13.8	37.0	10.6	17.2			0.21		256	192
5b	12.7	23.5	12.0	17.1			0.17		236	157
5c	12.7	17.0	14.1	17.0			0.15		235	171
5d	12.3	12.4	16.0	17.2			0.12		229	179
6	21.1	84.9	13.2	16.9			0.26	0.37 × 0.13	392	296
7	12.8	42.8	8.8	18.3			0.24	0.37 × 0.11	237	349
8	13.7	50.5	9.0	17.2			0.25	0.21 × 0.07	254	314
9	10.5	3.5	26.8	17.4			0.06	0.09 × 0.06	195	138
10	14.6	26.9	13.7	17.7			0.17	0.40 × 0.13	270	255
11	26.0	34.9	28.9	17.7			0.15		483	394
12	10.2	8.5	14.7	17.3			0.11		189	128
13	11.8	11.9	15.4	17.4			0.12		219	144
Mean	**14.1 ± 1.0**	**31 ± 6**	**15 ± 1**	**17.4 ± 0.09**			**0.17 ± 0.02**		**262 ± 19**	**243 ± 23**
Condensations										
1	32.6	21.9	53.5	14.4			0.10		605	110
2	26.3	8.8	67.0	15.1			0.06		488	123
3	29.8	49.8	29.4	15.3			0.16		552	122
4	32.4	21.7	53.1	15.5			0.10		601	168
5	42.4	21.3	82.7	15.1			0.08		787	156
6	59.3	69.5	70.9	15.1			0.14		1100	272
7	25.0	30.0	30.0	15.3			0.14		465	131
Mean	**35.4 ± 4.5**	**35 ± 5**	**55 ± 8**	**15.1 ± 0.1**			**0.11 ± 0.01**		**657 ± 84**	**155 ± 21**

Notes. The last line of each section gives the average (mean) values for each class of sources in bold. (1) Average column density derived within the 70 μm contour level. (2) Mass derived from column density map within the contours of the 70 μm data. (3) Average density from the mass M, assuming a spherical shape with an equivalent radius r. (4) Average temperature (average across the area covered by the 70 μm contour). (5) And (6) Minimum and maximum temperature. (7) Equivalent radius ($r = \sqrt{area/\pi}$), deconvolved with the beam (6″ for 70 μm that corresponds to 0.04 pc for a distance of 1.4 kpc). (8) Length and width for pillars (this study) and proplyd-like (sizes from Wright et al. 2012). (9) Surface density. (10) Average UV-flux in units of Habing field.

Theory and Simulations

Classical view

1. Radiation-driven implosion, i.e. large-scale compression of an expanding HII region on a molecular cloud surface creates **pillars** that then evolve into **globules** *(Bertoldi & McKee 1990; Lefoch & Lazareff 1994; Williams et al. 2001, …..)***.**

2. Hydrodynamic instabilities such as **Rayleigh-Taylor**, i.e. an instability of an interface between two fluids of different densities *(e.g. Mizuta et al. 2006).*

Turbulence and Geometry

Dense, primordial filaments are shaped by UV radiation into the form of pillars that then fragment under the influence of radiation into globules *(Dale et al. 2014).*

Turbulent density structure of molecular clouds can lead to local **curvatures** of the dense shell formed by the ionization compression, which develop into pillars.
(e.g. Gritschneder et al. 2009; Tremblin et al. 2011, 2012a,b)

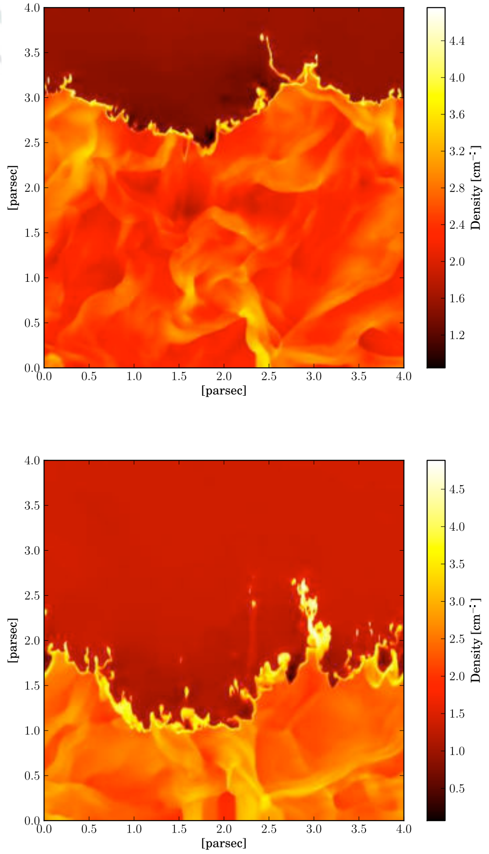

Simulations from Tremblin et al. 2012

Globule formation in simulations

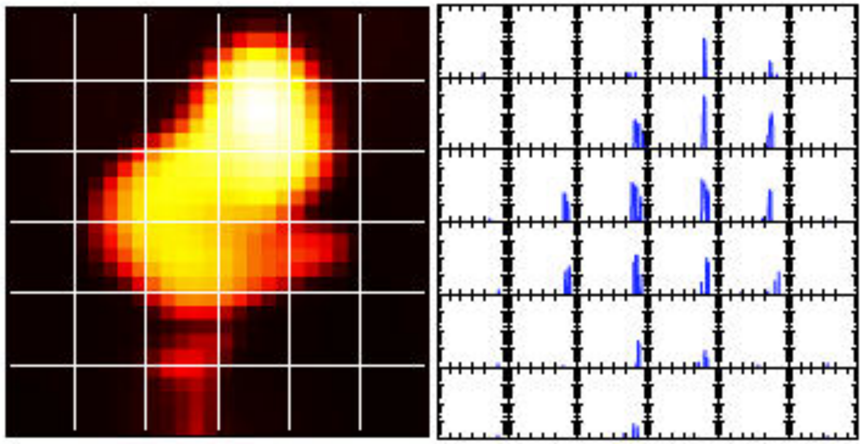

Predictions from numerical simulations
(Tremblin et al. 2011, 2012a,2012b, 2013)

Globules emerge from the radiation impacted, turbulent molecular cloud surface, they are not 'eroded' pillars.

Turbulent ram pressure of cold molecular gas must be higher than *ionization pressure.*

The globule does not need to have the same velocity as the ionizing gas or the molecular cloud.

The **velocity of a globule** is the signature of the initial turbulence.

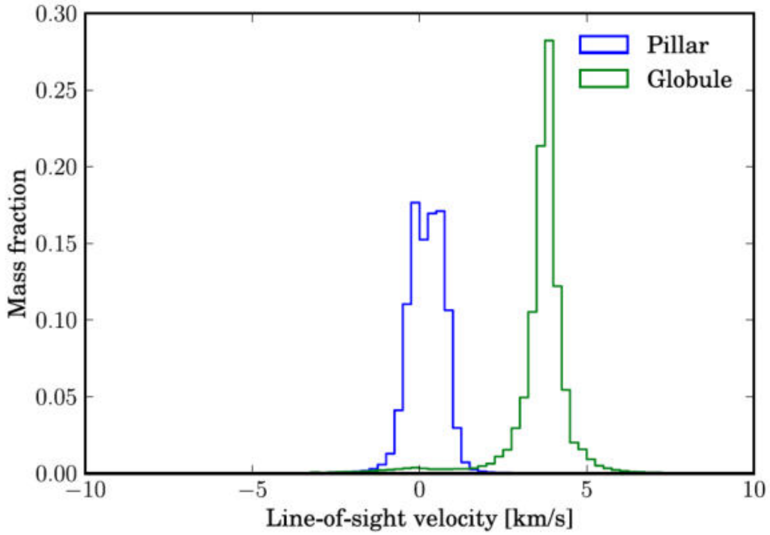

Globule formation in simulations

Walch et al. 2013:

Low fractal dimension: the border of the HII region is dominated by ***shell-like structures*** that break up into a a few massive high-density clumps.

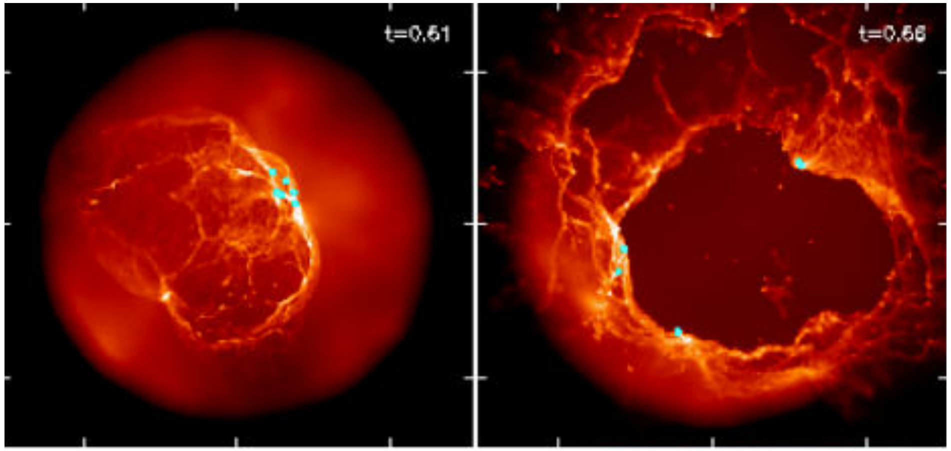

Column density at different time steps

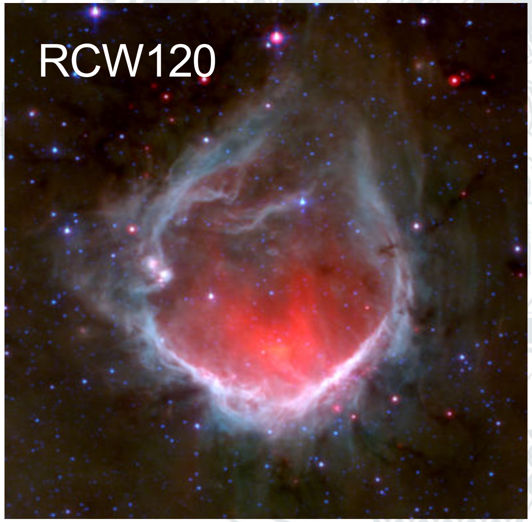

High fractal dimension: the border of the HII region is dominated by ***pillars*** and ***globules.***

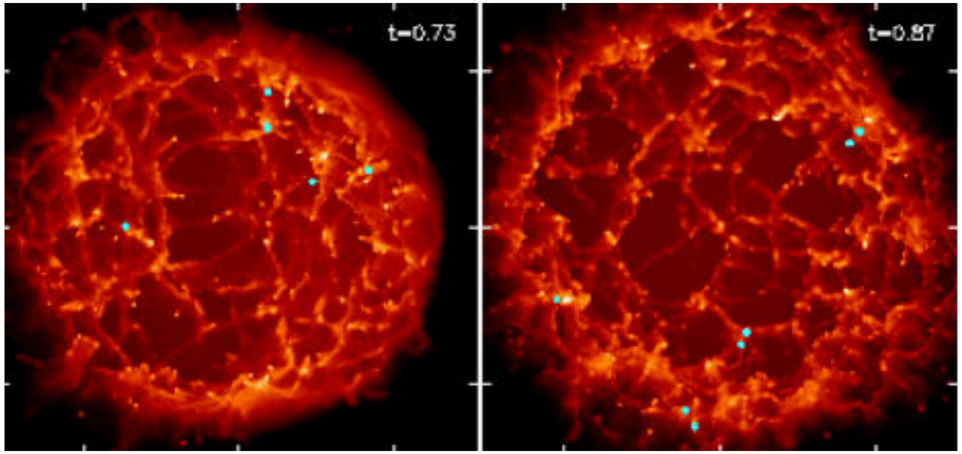

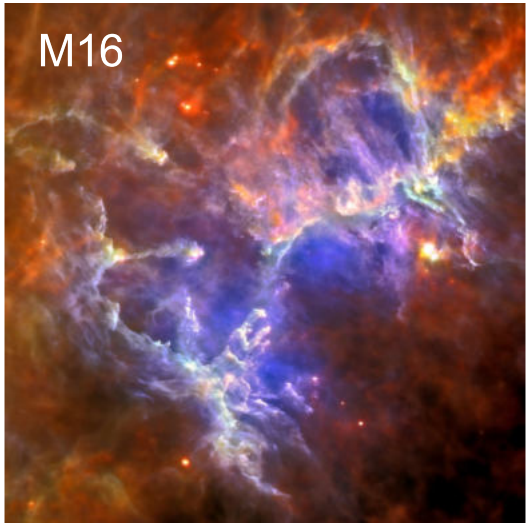

The Globule in Cygnus X

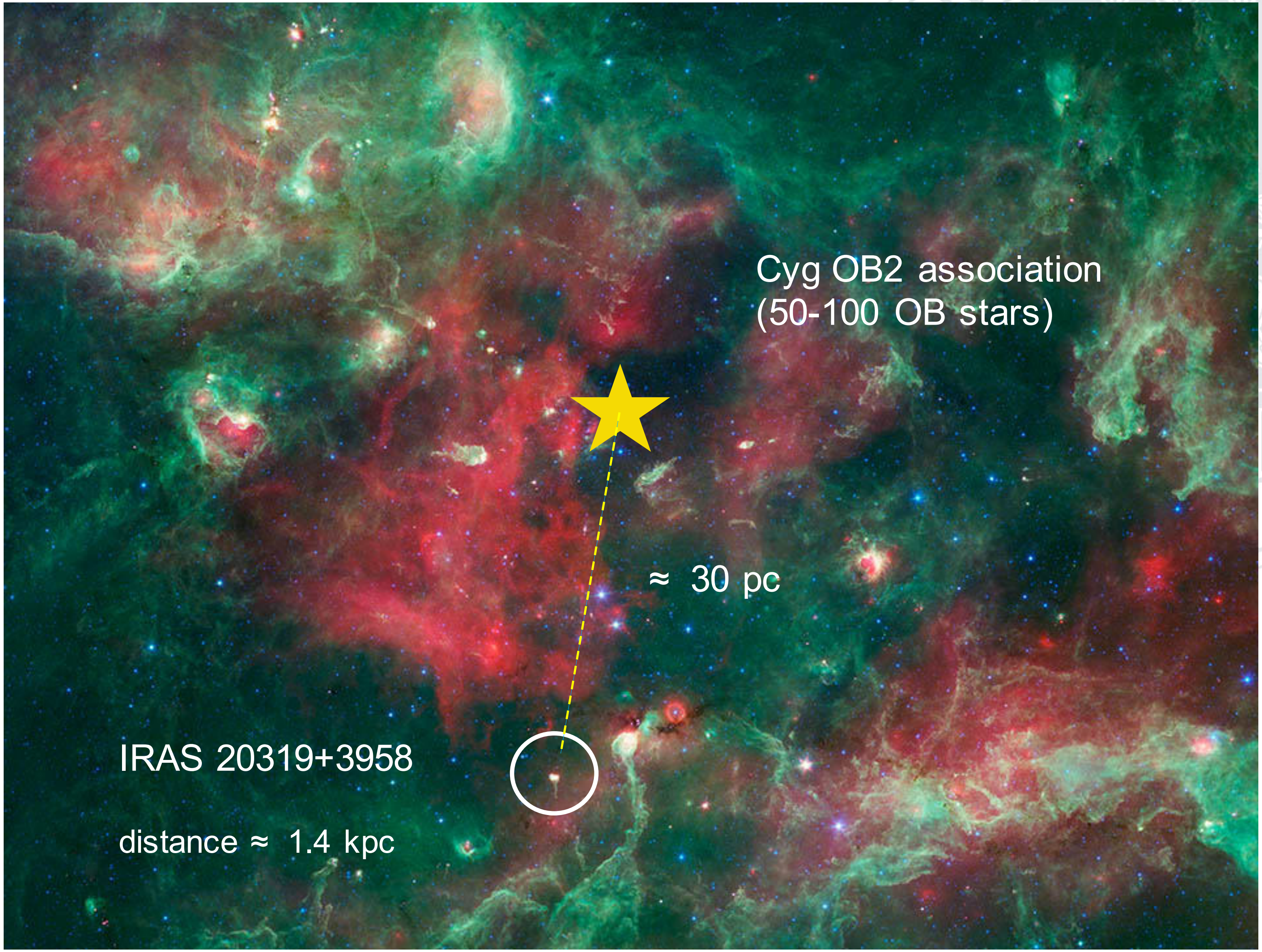

Spitzer Cygnus X legacy (Hora et al.)

The globule in CII: excitation external ? internal? both?

CII 158 μm SOFIA line integrated (0-15 km/s) intensity *(early science Schneider et al. 2012)*

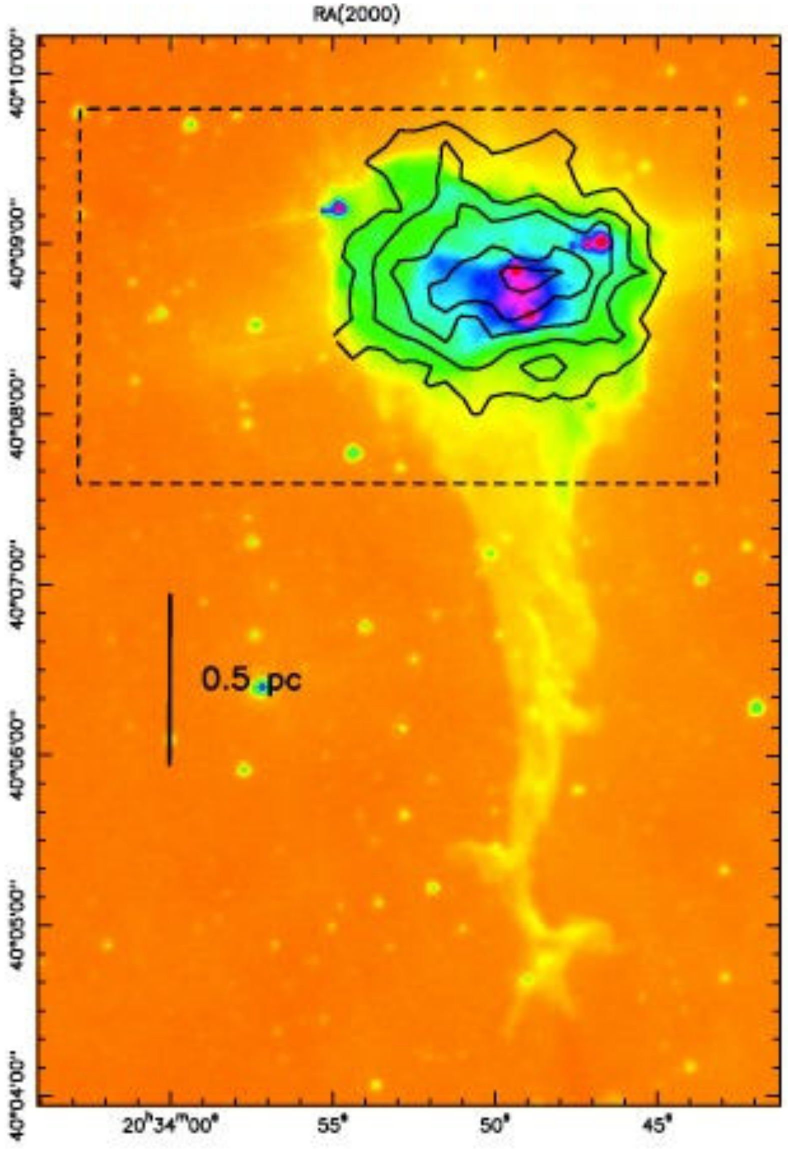

Spitzer IR 4.5 μm

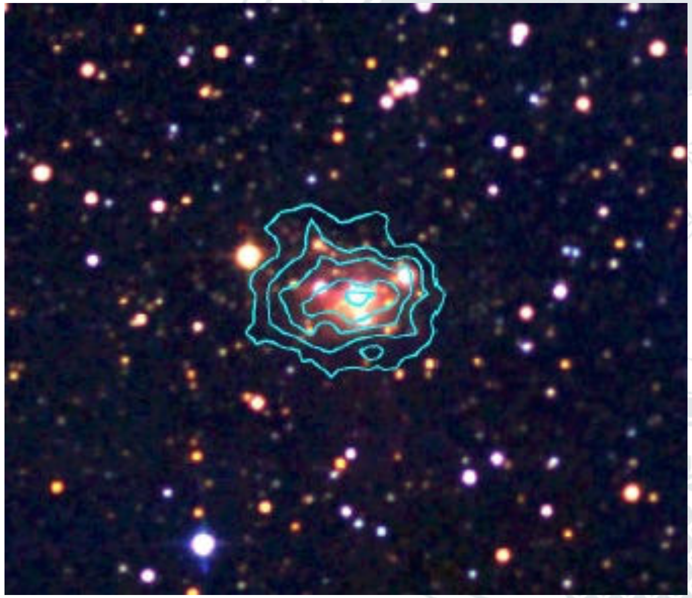

CII contours on 2MASS J, H, K image

2012: 'CII and ^{12}CO 11-10 emission from internal photodissociation regions (PDRs).'

-> need of careful PDR modelling to check !

(Herschel OT project PACS/SPIRE/HIFI in Cygnus, Rosette, M16)

Large set of FIR cooling lines

CII 158 μm Herschel/HIFI line integrated (0-15 km/s) intensity

▲ 'star A'

Binary, one Herbig Be star

□ 'star B'

B0.5 to B1.5

+ 'star C'

Binary, one late O or early B

+ young cluster with 30-40 stars

(Djupvik, Comeron, Schneider 2017)

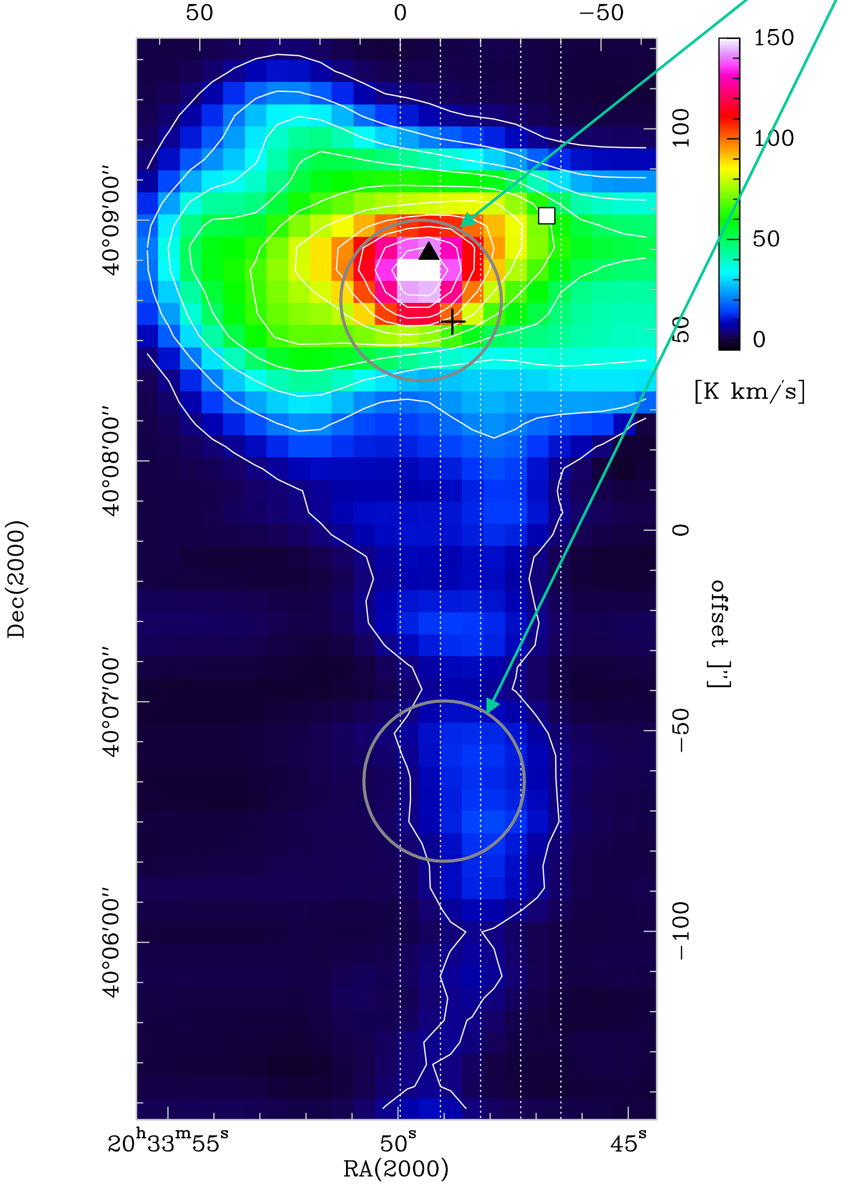

Schneider, Röllig et al. 2021

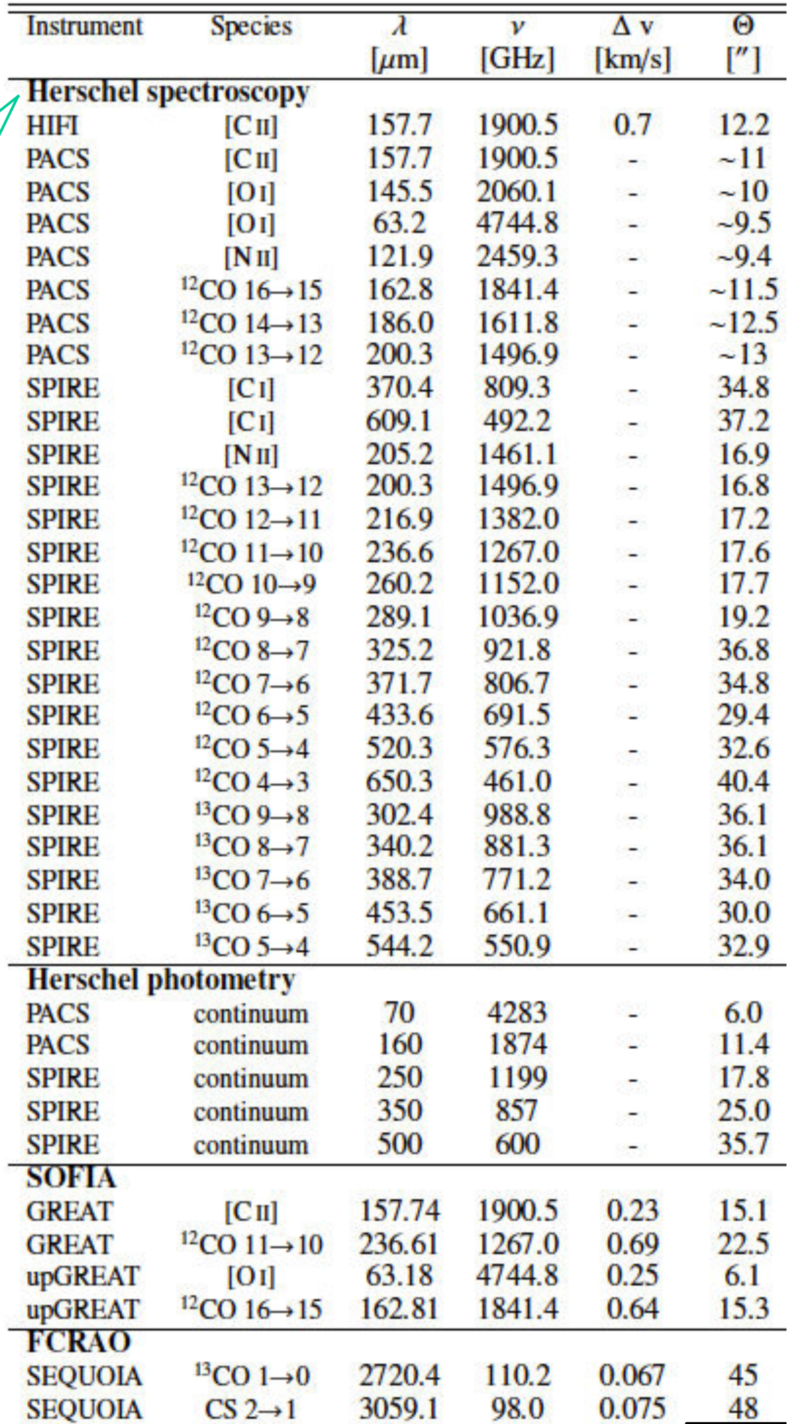

Instrument	Species	λ	ν	Δ v	Θ
		[μm]	[GHz]	[km/s]	['']
Herschel spectroscopy					
HIFI	[C II]	157.7	1900.5	0.7	12.2
PACS	[C II]	157.7	1900.5	-	~11
PACS	[O I]	145.5	2060.1	-	~10
PACS	[O I]	63.2	4744.8	-	~9.5
PACS	[N II]	121.9	2459.3	-	~9.4
PACS	^{12}CO 16→15	162.8	1841.4	-	~11.5
PACS	^{12}CO 14→13	186.0	1611.8	-	~12.5
PACS	^{12}CO 13→12	200.3	1496.9	-	~13
SPIRE	[C I]	370.4	809.3	-	34.8
SPIRE	[C I]	609.1	492.2	-	37.2
SPIRE	[N II]	205.2	1461.1	-	16.9
SPIRE	^{12}CO 13→12	200.3	1496.9	-	16.8
SPIRE	^{12}CO 12→11	216.9	1382.0	-	17.2
SPIRE	^{12}CO 11→10	236.6	1267.0	-	17.6
SPIRE	^{12}CO 10→9	260.2	1152.0	-	17.7
SPIRE	^{12}CO 9→8	289.1	1036.9	-	19.2
SPIRE	^{12}CO 8→7	325.2	921.8	-	36.8
SPIRE	^{12}CO 7→6	371.7	806.7	-	34.8
SPIRE	^{12}CO 6→5	433.6	691.5	-	29.4
SPIRE	^{12}CO 5→4	520.3	576.3	-	32.6
SPIRE	^{12}CO 4→3	650.3	461.0	-	40.4
SPIRE	^{13}CO 9→8	302.4	988.8	-	36.1
SPIRE	^{13}CO 8→7	340.2	881.3	-	36.1
SPIRE	^{13}CO 7→6	388.7	771.2	-	34.0
SPIRE	^{13}CO 6→5	453.5	661.1	-	30.0
SPIRE	^{13}CO 5→4	544.2	550.9	-	32.9
Herschel photometry					
PACS	continuum	70	4283	-	6.0
PACS	continuum	160	1874	-	11.4
SPIRE	continuum	250	1199	-	17.8
SPIRE	continuum	350	857	-	25.0
SPIRE	continuum	500	600	-	35.7
SOFIA					
GREAT	[C II]	157.74	1900.5	0.23	15.1
GREAT	^{12}CO 11→10	236.61	1267.0	0.69	22.5
upGREAT	[O I]	63.18	4744.8	0.25	6.1
upGREAT	^{12}CO 16→15	162.81	1841.4	0.64	15.3
FCRAO					
SEQUOIA	^{13}CO 1→0	2720.4	110.2	0.067	45
SEQUOIA	CS 2→1	3059.1	98.0	0.075	48
JCMT					
HARP	^{12}CO 3→2	869.0	345.8	0.42	

Large set of FIR cooling lines

SPIRE velocity unresolved lines from the Globule head position

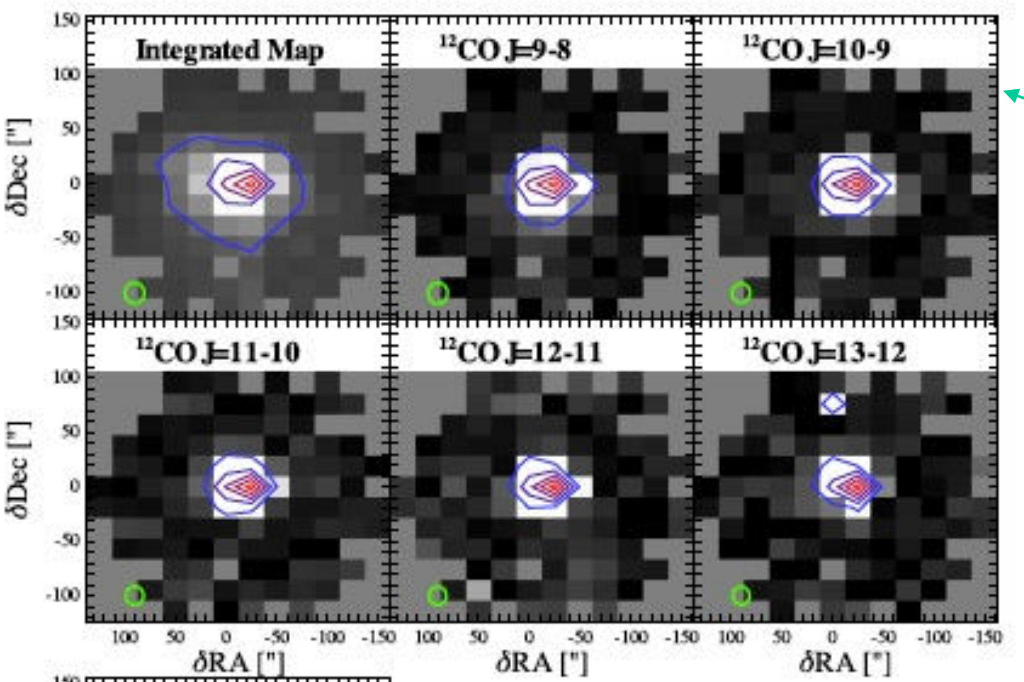

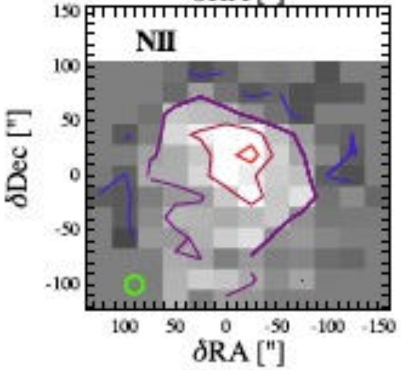

Schneider, Röllig, Polehampton et al. 2021

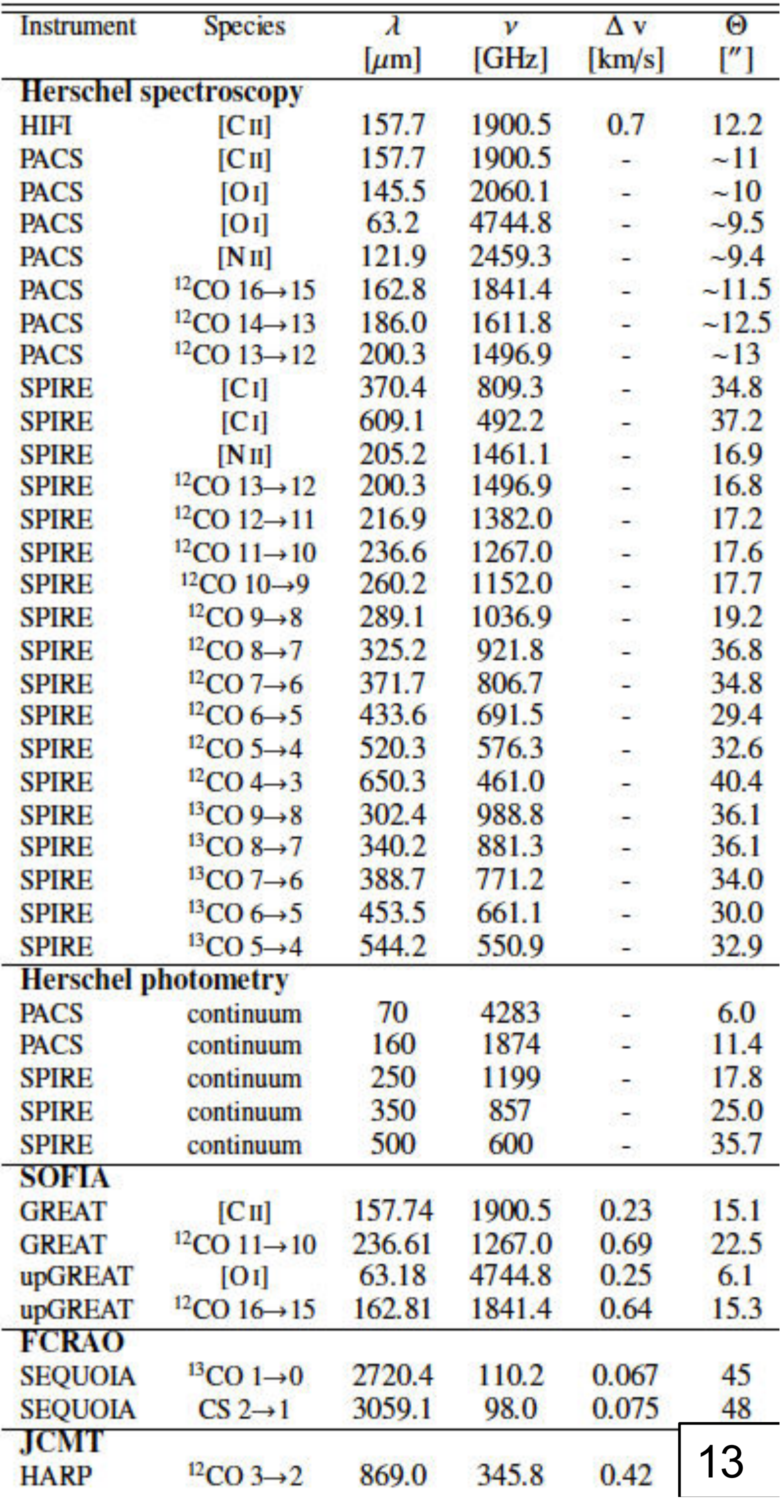

Instrument	Species	λ [μm]	ν [GHz]	Δ v [km/s]	Θ ["]
Herschel spectroscopy					
HIFI	[C II]	157.7	1900.5	0.7	12.2
PACS	[C II]	157.7	1900.5	-	~11
PACS	[O I]	145.5	2060.1	-	~10
PACS	[O I]	63.2	4744.8	-	~9.5
PACS	[N II]	121.9	2459.3	-	~9.4
PACS	^{12}CO 16→15	162.8	1841.4	-	~11.5
PACS	^{12}CO 14→13	186.0	1611.8	-	~12.5
PACS	^{12}CO 13→12	200.3	1496.9	-	~13
SPIRE	[C I]	370.4	809.3	-	34.8
SPIRE	[C I]	609.1	492.2	-	37.2
SPIRE	[N II]	205.2	1461.1	-	16.9
SPIRE	^{12}CO 13→12	200.3	1496.9	-	16.8
SPIRE	^{12}CO 12→11	216.9	1382.0	-	17.2
SPIRE	^{12}CO 11→10	236.6	1267.0	-	17.6
SPIRE	^{12}CO 10→9	260.2	1152.0	-	17.7
SPIRE	^{12}CO 9→8	289.1	1036.9	-	19.2
SPIRE	^{12}CO 8→7	325.2	921.8	-	36.8
SPIRE	^{12}CO 7→6	371.7	806.7	-	34.8
SPIRE	^{12}CO 6→5	433.6	691.5	-	29.4
SPIRE	^{12}CO 5→4	520.3	576.3	-	32.6
SPIRE	^{12}CO 4→3	650.3	461.0	-	40.4
SPIRE	^{13}CO 9→8	302.4	988.8	-	36.1
SPIRE	^{13}CO 8→7	340.2	881.3	-	36.1
SPIRE	^{13}CO 7→6	388.7	771.2	-	34.0
SPIRE	^{13}CO 6→5	453.5	661.1	-	30.0
SPIRE	^{13}CO 5→4	544.2	550.9	-	32.9
Herschel photometry					
PACS	continuum	70	4283	-	6.0
PACS	continuum	160	1874	-	11.4
SPIRE	continuum	250	1199	-	17.8
SPIRE	continuum	350	857	-	25.0
SPIRE	continuum	500	600	-	35.7
SOFIA					
GREAT	[C II]	157.74	1900.5	0.23	15.1
GREAT	^{12}CO 11→10	236.61	1267.0	0.69	22.5
upGREAT	[O I]	63.18	4744.8	0.25	6.1
upGREAT	^{12}CO 16→15	162.81	1841.4	0.64	15.3
FCRAO					
SEQUOIA	^{13}CO 1→0	2720.4	110.2	0.067	45
SEQUOIA	CS 2→1	3059.1	98.0	0.075	48
JCMT					
HARP	^{12}CO 3→2	869.0	345.8	0.42	

The globule is rotating see SOFIA CII map of globule head, *Schneider et al. (2012)*

CII integrated intensity

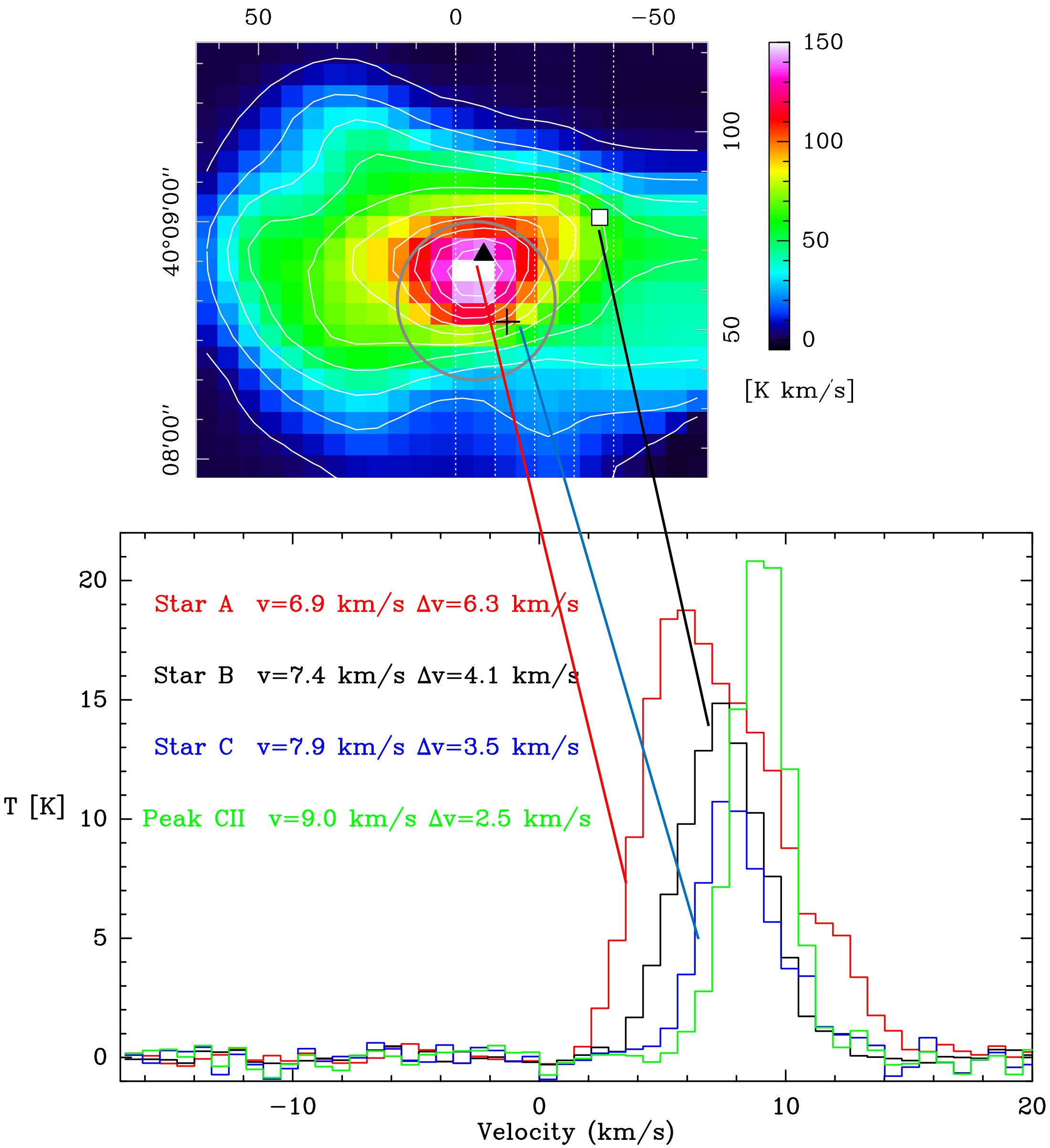

CII velocity

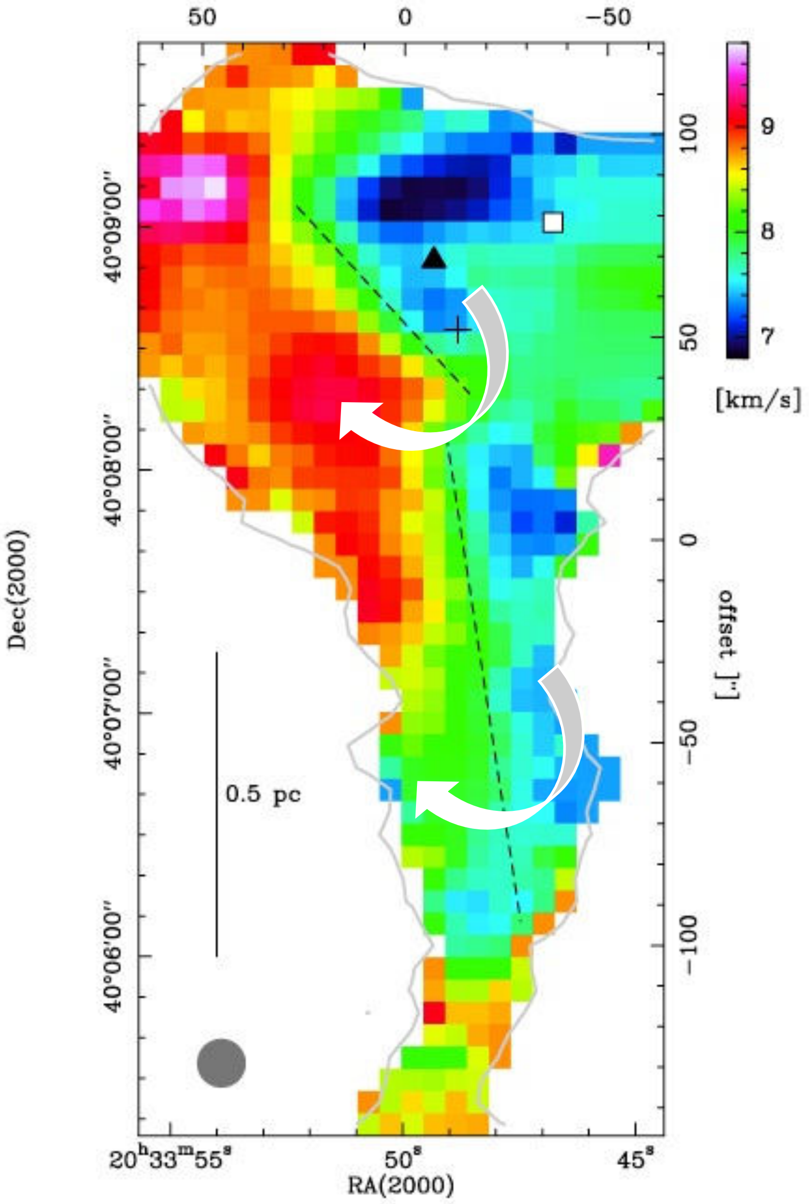

Solid body rotation?

$M = (v^2 r) / G$ Minimum mass needed to support rotation

Globule head:
$v \sim 0.2$ km/s , $r \sim 0.1$-0.2 pc

-> $M \sim 100\ M_{sun}$

Mass from dust column density ~ 170 M_{sun}

Did the globule get a 'kick' (= momentum) when it detached from the molecular cloud?

Magnetic fields (helix model, *Gahm et al. 2006*)?

Do stellar feedback effects (radiation, winds) provoke the rotation?

A CII ‚outflow‘

‘Star A’:
Two components with one early-B type
(Herbig Be, possibly type III)

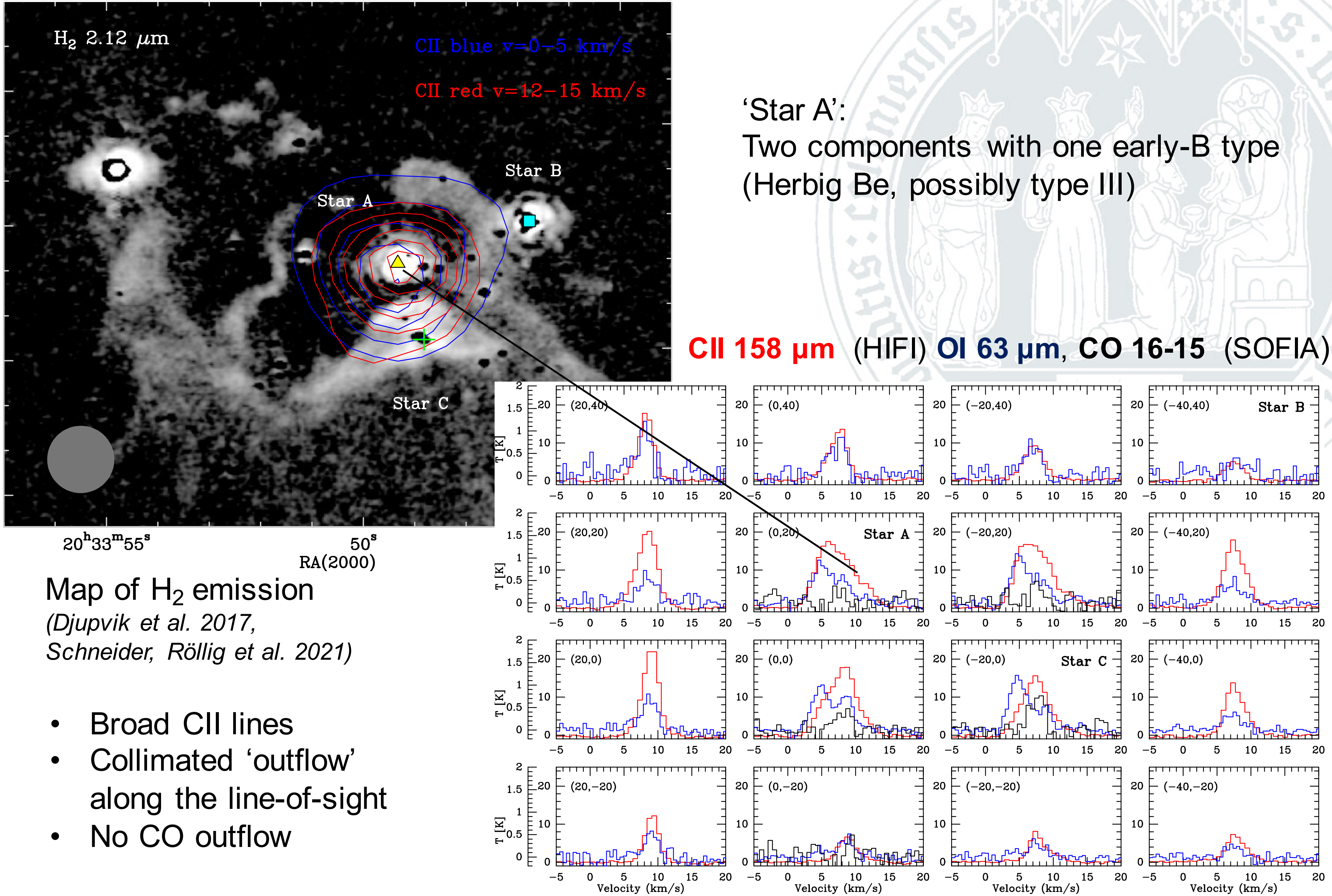

CII 158 µm (HIFI) **OI 63 µm**, **CO 16-15** (SOFIA)

Map of H$_2$ emission
(Djupvik et al. 2017,
Schneider, Röllig et al. 2021)

- Broad CII lines
- Collimated ‘outflow’ along the line-of-sight
- No CO outflow

A CII outflow driven by a Herbig Be star?

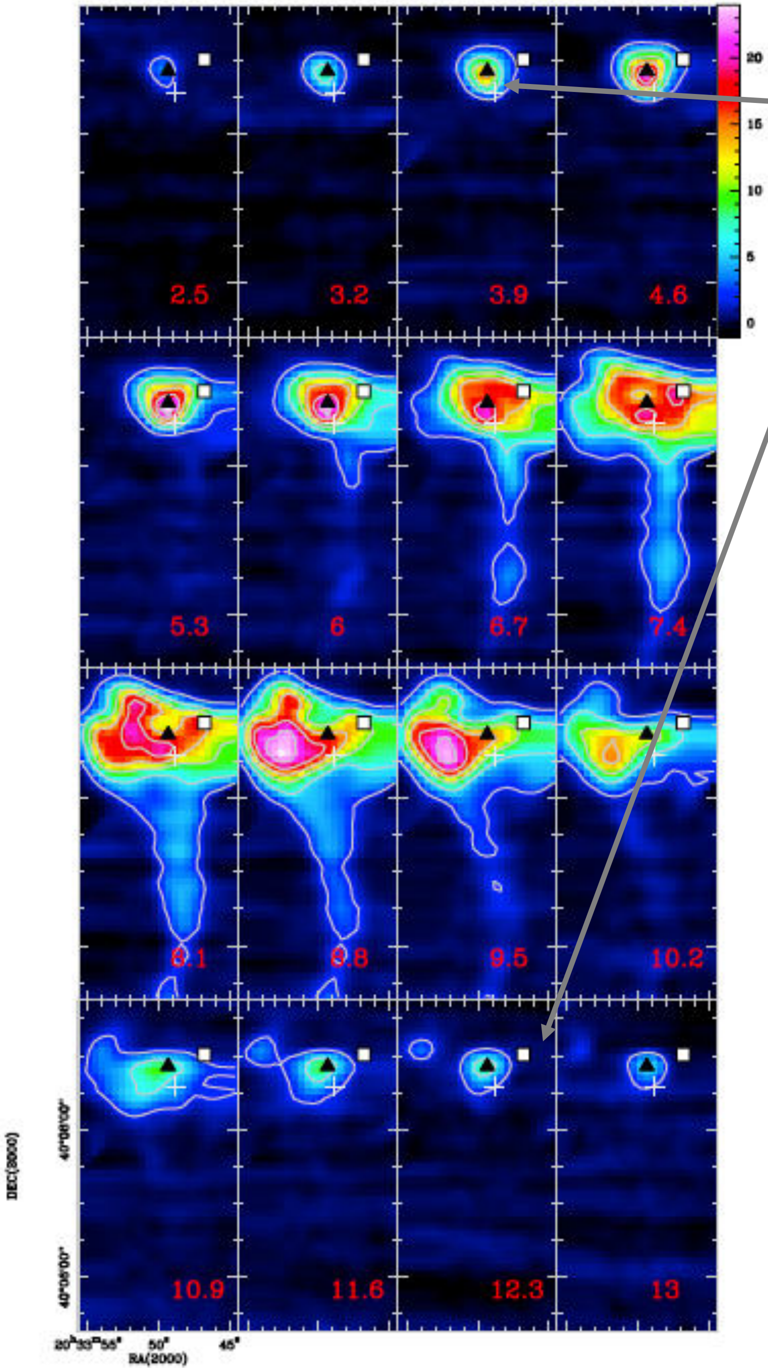

CII 'outflow' in channel maps, no promiment OI 63 μm wings -> no shocks? But prominent H_2 emission..

YSO outflow driven by the stellar wind or magneto-centrifugally star-disk interaction? *(Cauley & Johns-Krull 2014; Moura et al. 2020; Rodriguez et al. 2014)*

'Outflowing gas' from ablation of the photodissociation region of the cavity walls? *(see S106, Schneider et al. 2018)*

PDR modelling – Complexity

Geometry
- plane parallel slab
- sphere (new parameter: mass)
- circular paraboloid (outflow)
- 3-D, clumpy, fractal

Radiation field (int & ext)
- isotropic and/or directed/inclined
- spectral shape of FUV field
  - physics and chemistry: f(λ)
- detailed photon cross-section
- line-overlap, scattering,…

Dust content („terra incognita“)
- dust composition, size distribution ?
- very small grains, PAHs, PE efficiency,
  charge exchange
- grain surface: sticking, E_{des}, …

Chemistry
- Large nonlinear chemical networks
  ~10-20% reaction rates known
- coupling to heating & cooling & RT
- ice & surface & gas chemistry
- coupling to FUV & CR & XR
- state-to-state reaction rates

Energetics / Thermodynamics
- couples to FUV RT & dust &chemistry
- full treatment of H_2,HD,CO,H_2O,….
- detailed internal RT vs. approx.
- chemical heating & cooling
- multi-stability solutions?

Stationarity
- stationary vs. time-dep solution
- initial conditions?
- rate uncertainties more important
- UV field, geometry, pressure/density

Numerics
- non-linear coupling of geometry RT & energetics & chemistry
- scaling with chemistry: $N^{3.5}$
- interpolation → uncertainties
- n-dim global root search
- multiple solutions !?

PDR modelling.....

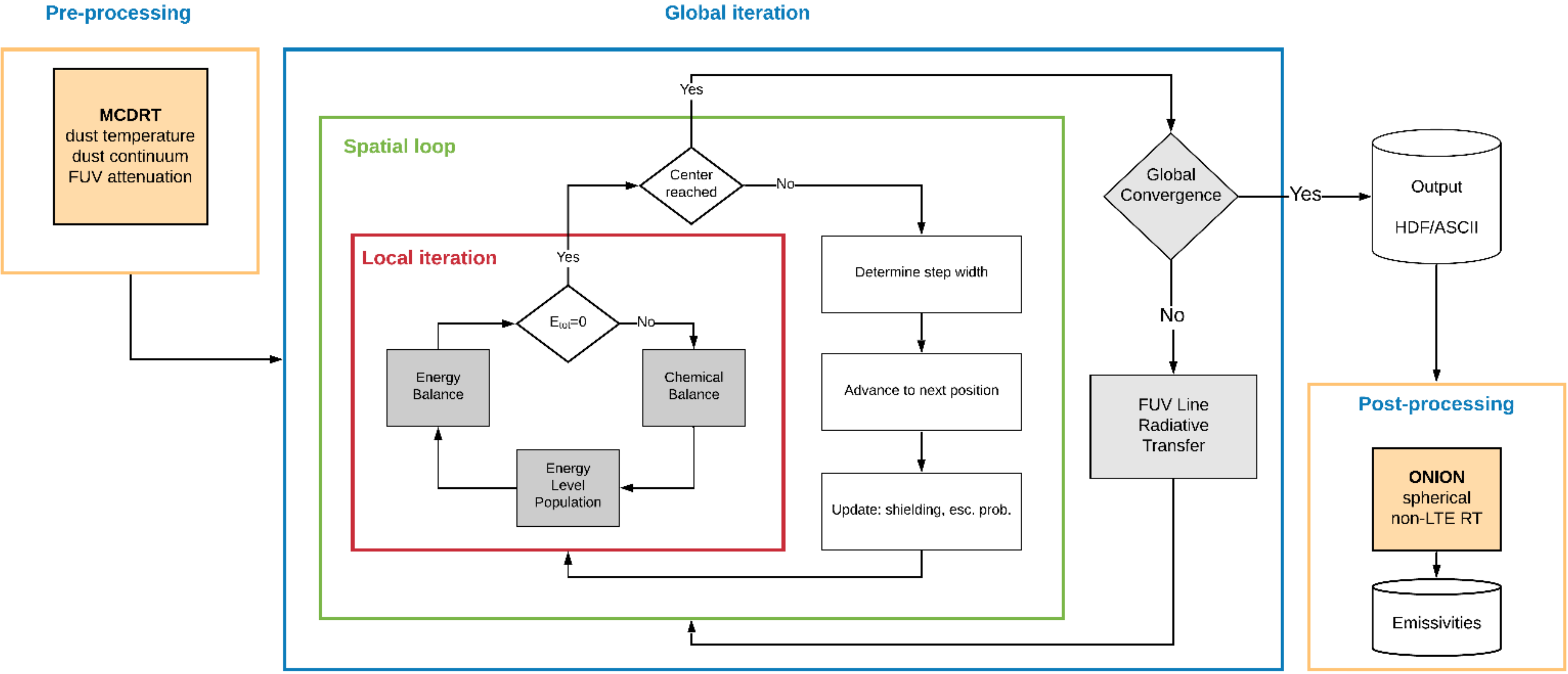

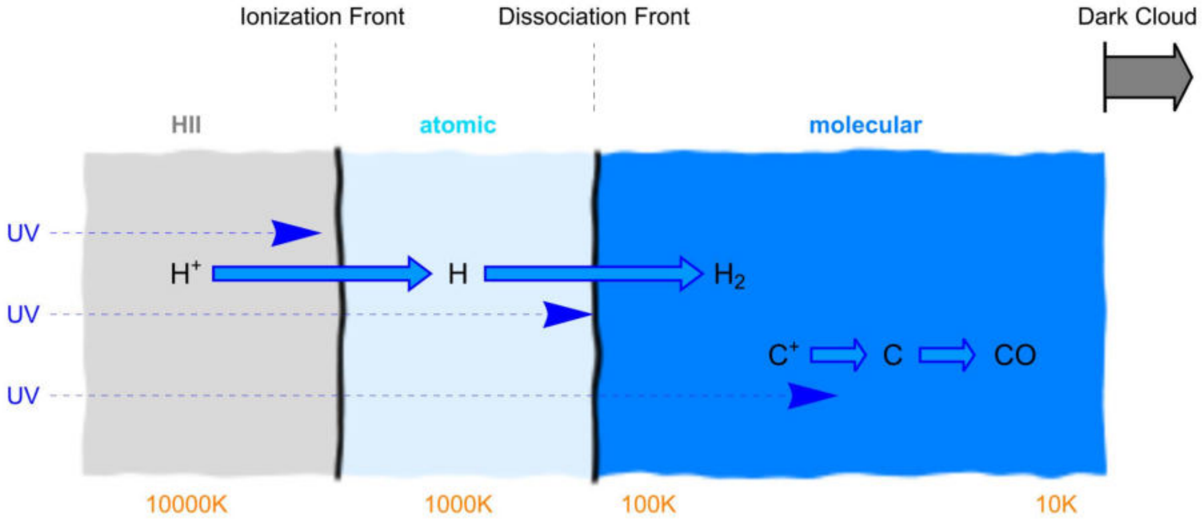

PDR modelling – KOSMA-τ

- 1-D, spherical geometry
  - power-law density profile
  - isotropic illumination
- self-consistent solution of energy balance, chemistry and radiative transfer
- self-shielding of H_2, CO
- detailed dust treatment: $I_{UV}(\lambda)$, T_{dust}, dn/da,..
- 3-phase chemistry (gas – ice – surface)
- Full H_2 ro-vib treatment
- Non-LTE RT: clump emission
- clumpy cloud composition
  - stochastic clump ensemble
  - KOSMA-τ 3D (Andree-Labsch et al. 2017)

COMING SOON

- Online database and Python interface
  - PDR Toolbox – pdrtpy http://dustem.astro.umd.edu/
  - InterStellar Medium DataBase (**ISMDB**) https://ism.obspm.fr

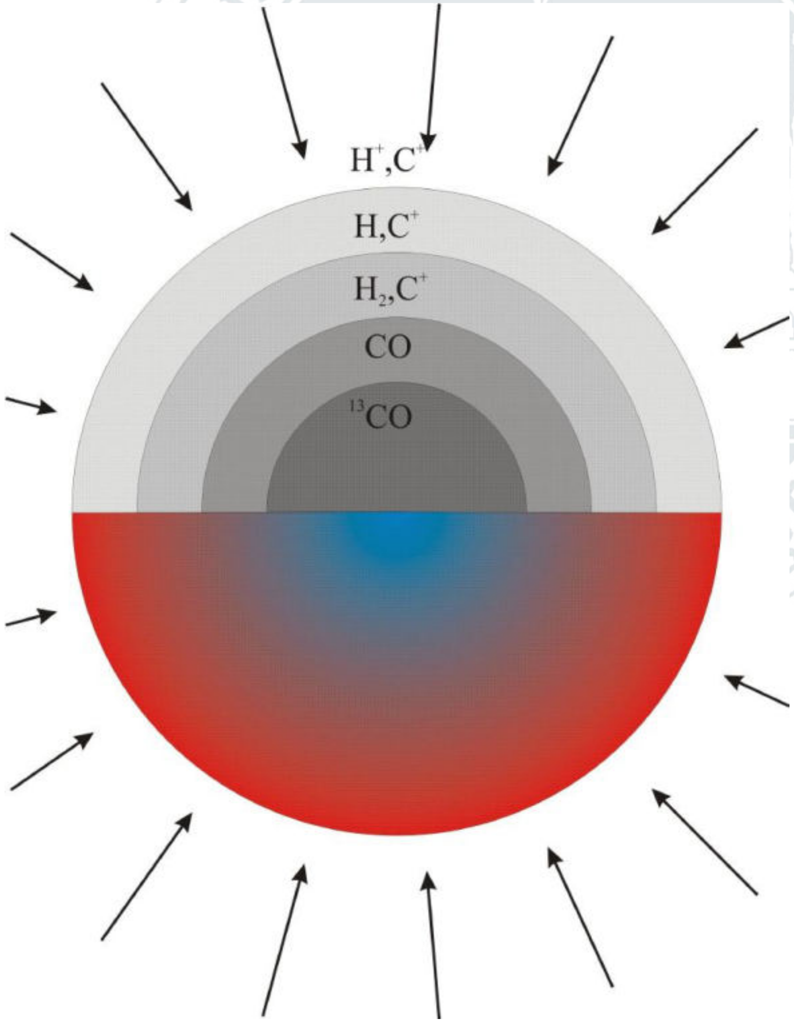

PDR modelling – KOSMA-τ

- 1-D, spherical geometry
  - power-law density profile
  - isotropic illumination
- self-consistent solution of energy balance, chemistry and radiative transfer
- self-shielding of H_2, CO
- detailed dust treatment: $I_{UV}(\lambda)$, T_{dust}, dn/da,
- 3-phase chemistry (gas – ice – surface)
- Full H_2 ro-vib treatment
- Non-LTE RT: clump emission
- clumpy cloud composition
  - stochastic clump ensemble
  - KOSMA-τ 3D (Andree-Labsch et al. 2017)

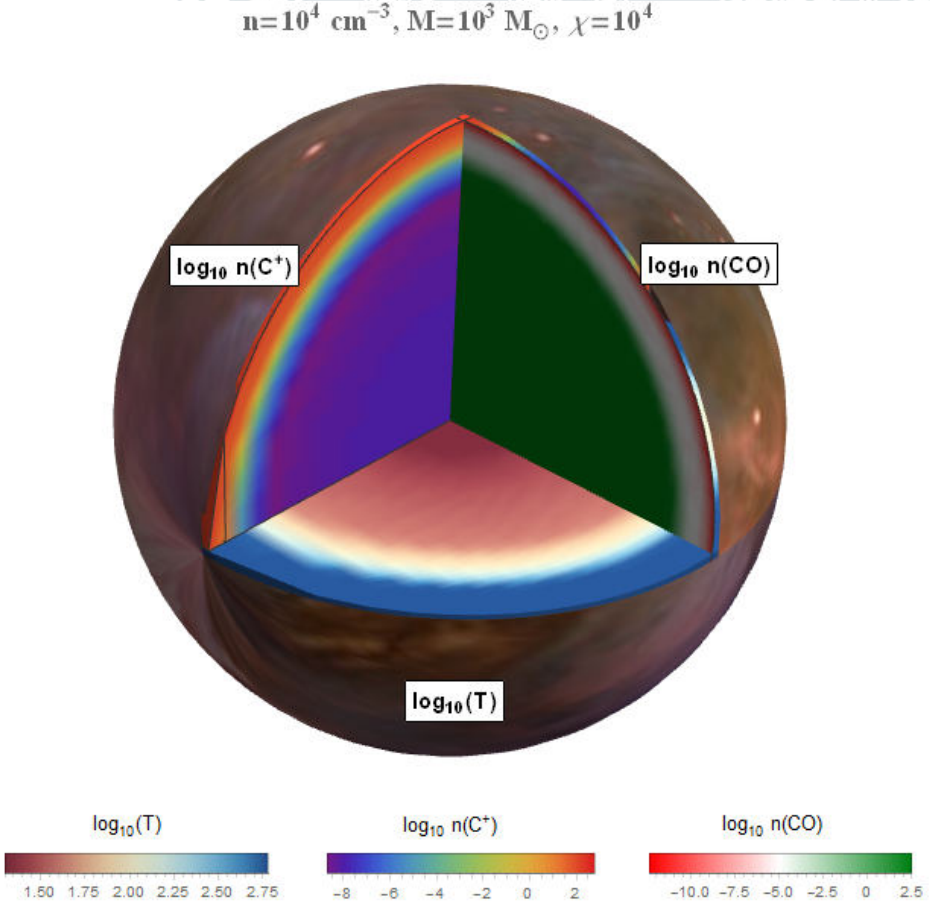

COMING SOON

- Online database and Python interface
  - PDR Toolbox – pdrtpy http://dustem.astro.umd.edu/
  - InterStellar Medium DataBase (**ISMDB**) https://ism.obspm.fr

PDR modelling – KOSMA-τ

- 1-D, spherical geometry
  - power-law density profile
  - isotropic illumination
- self-consistent solution of energy balance, chemistry and radiative transfer
- self-shielding of H_2, CO
- detailed dust treatment: $I_{UV}(\lambda)$, T_{dust}, dn/da,..
- 3-phase chemistry (gas – ice – surface)
- Full H_2 ro-vib treatment
- Non-LTE RT: clump emission
- clumpy cloud composition
  - stochastic clump ensemble
  - KOSMA-τ 3D (Andree-Labsch et al. 2017)

COMING SOON

- Online database and Python interface
  - PDR Toolbox – pdrtpy http://dustem.astro.umd.edu/
  - InterStellar Medium DataBase (**ISMDB**) https://ism.obspm.fr

Background Rosette (*Herschel*, Motte et al. 2010, Schneider et al. 2010)

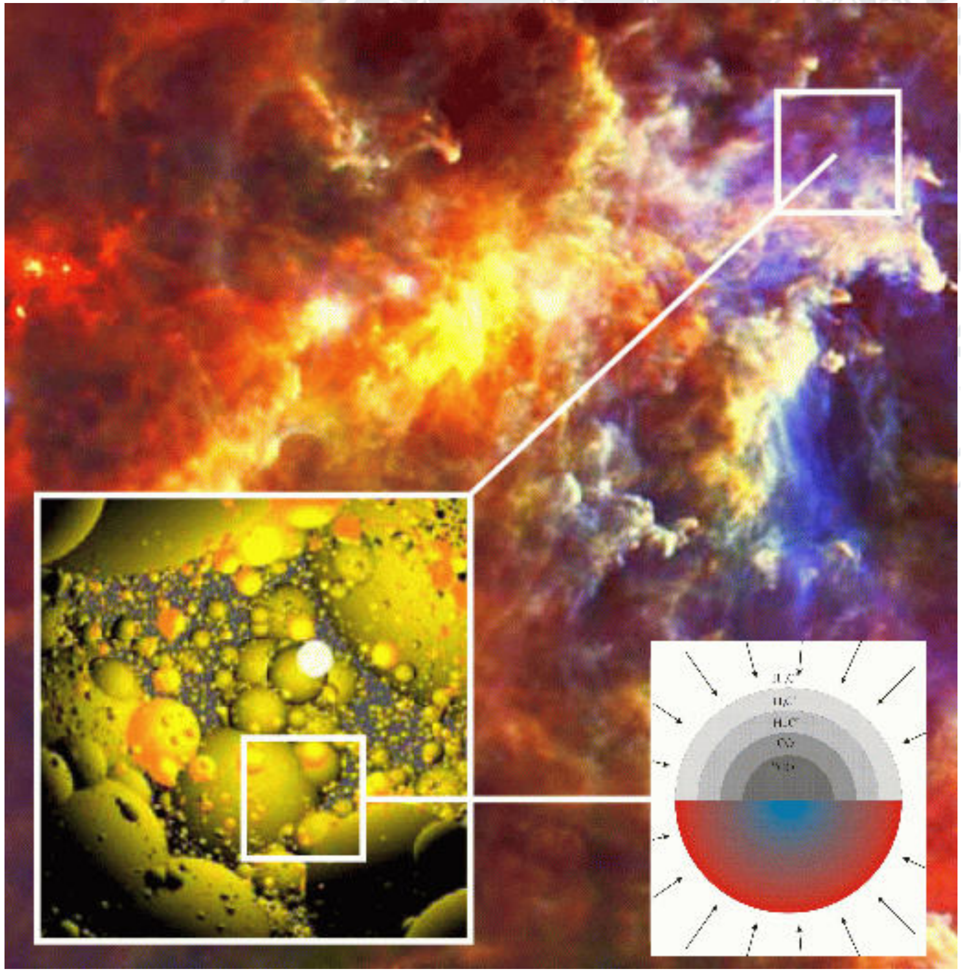

PDR modelling – KOSMA-τ

- 1-D, spherical geometry
    - power-law density profile
    - isotropic illumination
- self-consistent solution of energy balance, chemistry and radiative transfer
- self-shielding of H_2, CO
- detailed dust treatment: $I_{UV}(\lambda)$, T_{dust}, dn/da,..
- 3-phase chemistry (gas – ice – surface)
- Full H_2 ro-vib treatment
- Non-LTE RT: clump emission
- clumpy cloud composition
    - stochastic clump ensemble
    - KOSMA-τ 3D (Andree-Labsch et al. 2017)

COMING SOON

- Online database and Python interface
    - PDR Toolbox – pdrtpy http://dustem.astro.umd.edu/
    - InterStellar Medium DataBase (**ISMDB**) https://ism.obspm.fr

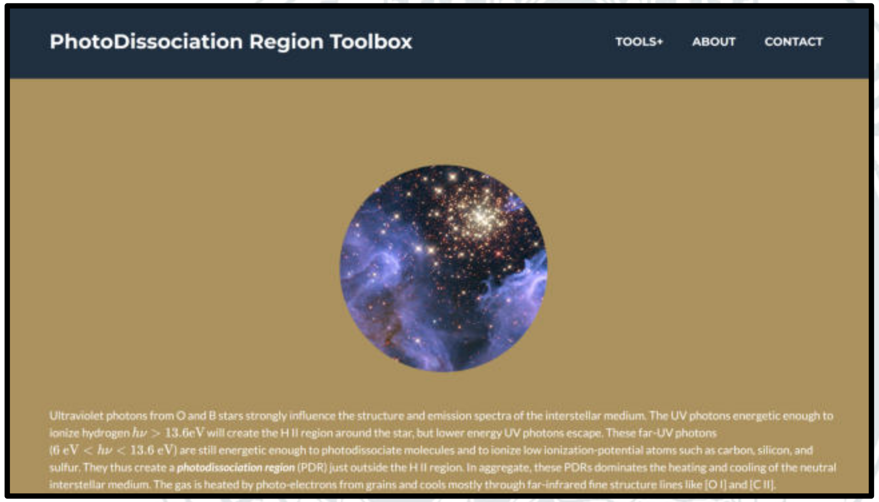

Ultraviolet photons from O and B stars strongly influence the structure and emission spectra of the interstellar medium. The UV photons energetic enough to ionize hydrogen $h\nu > 13.6\mathrm{eV}$ will create the H II region around the star, but lower energy UV photons escape. These far-UV photons ($6\ \mathrm{eV} < h\nu < 13.6\ \mathrm{eV}$) are still energetic enough to photodissociate molecules and to ionize low ionization-potential atoms such as carbon, silicon, and sulfur. They thus create a ***photodissociation region*** (PDR) just outside the H II region. In aggregate, these PDRs dominates the heating and cooling of the neutral interstellar medium. The gas is heated by photo-electrons from grains and cools mostly through far-infrared fine structure lines like [O I] and [C II].

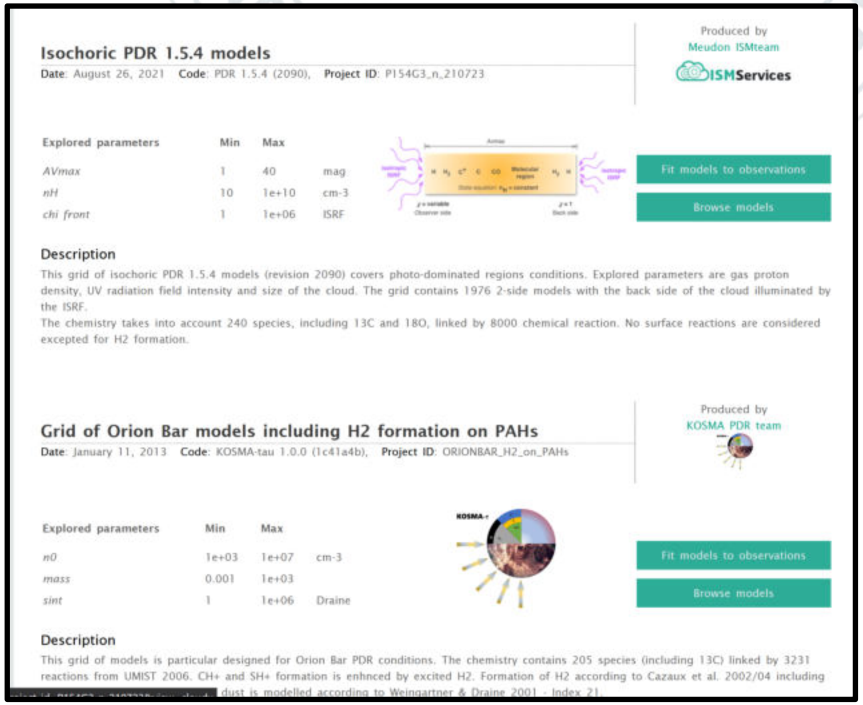

Isochoric PDR 1.5.4 models

Date: August 26, 2021 **Code**: PDR 1.5.4 (2090), **Project ID**: P154G3_n_210723

Explored parameters	Min	Max	
AVmax	1	40	mag
nH	10	1e+10	cm-3
chi front	1	1e+06	ISRF

Description

This grid of isochoric PDR 1.5.4 models (revision 2090) covers photo-dominated regions conditions. Explored parameters are gas proton density, UV radiation field intensity and size of the cloud. The grid contains 1976 2-side models with the back side of the cloud illuminated by the ISRF.

The chemistry takes into account 240 species, including 13C and 18O, linked by 8000 chemical reaction. No surface reactions are considered excepted for H2 formation.

Grid of Orion Bar models including H2 formation on PAHs

Date: January 11, 2013 **Code**: KOSMA-tau 1.0.0 (1c41a4b), **Project ID**: ORIONBAR_H2_on_PAHs

Explored parameters	Min	Max	
n0	1e+03	1e+07	cm-3
mass	0.001	1e+03	
sint	1	1e+06	Draine

Description

This grid of models is particular designed for Orion Bar PDR conditions. The chemistry contains 205 species (including 13C) linked by 3231 reactions from UMIST 2006. CH+ and SH+ formation is enhnced by excited H2. Formation of H2 according to Cazaux et al. 2002/04 including dust is modelled according to Weingartner & Draine 2001 - Index 21

A physical model of the globule

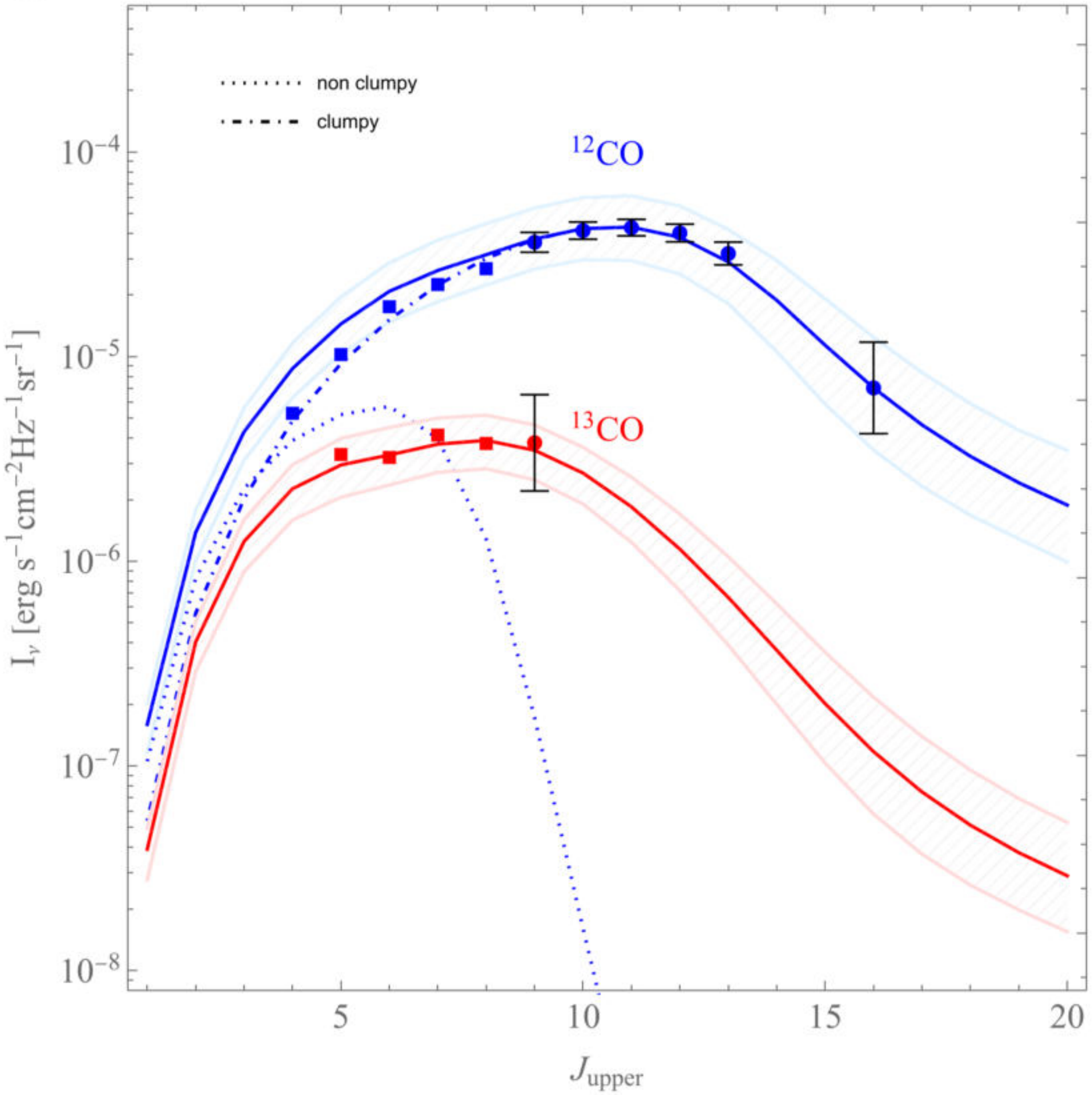

CO-SLED: spectral line energy distribution

2-component model gives best fit

PDR modelling of the head

FUV field estimated from

1. Herschel fluxes 70, 160 µm

$$F_{\rm fuv}[G_0] = (4\pi I_{\rm FIR}\,1000)/1.6.$$

2. Star properties ($T_{\rm eff}$, L)

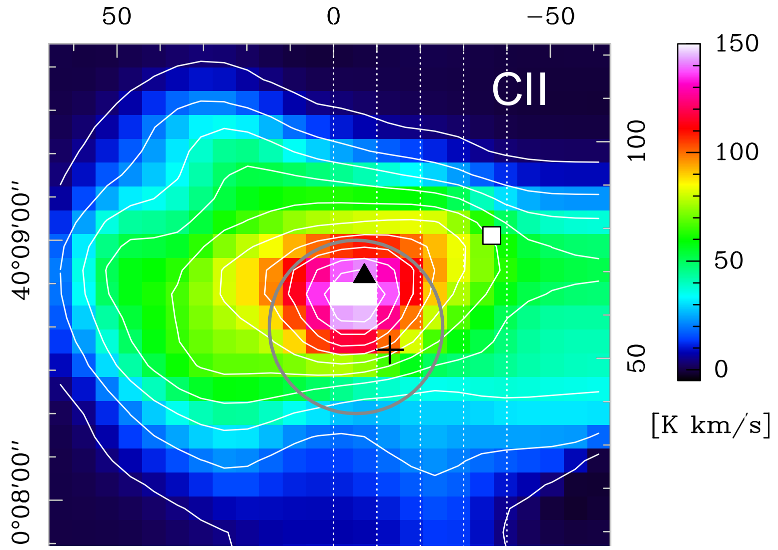

A physical model of the globule   PDR modelling of the head

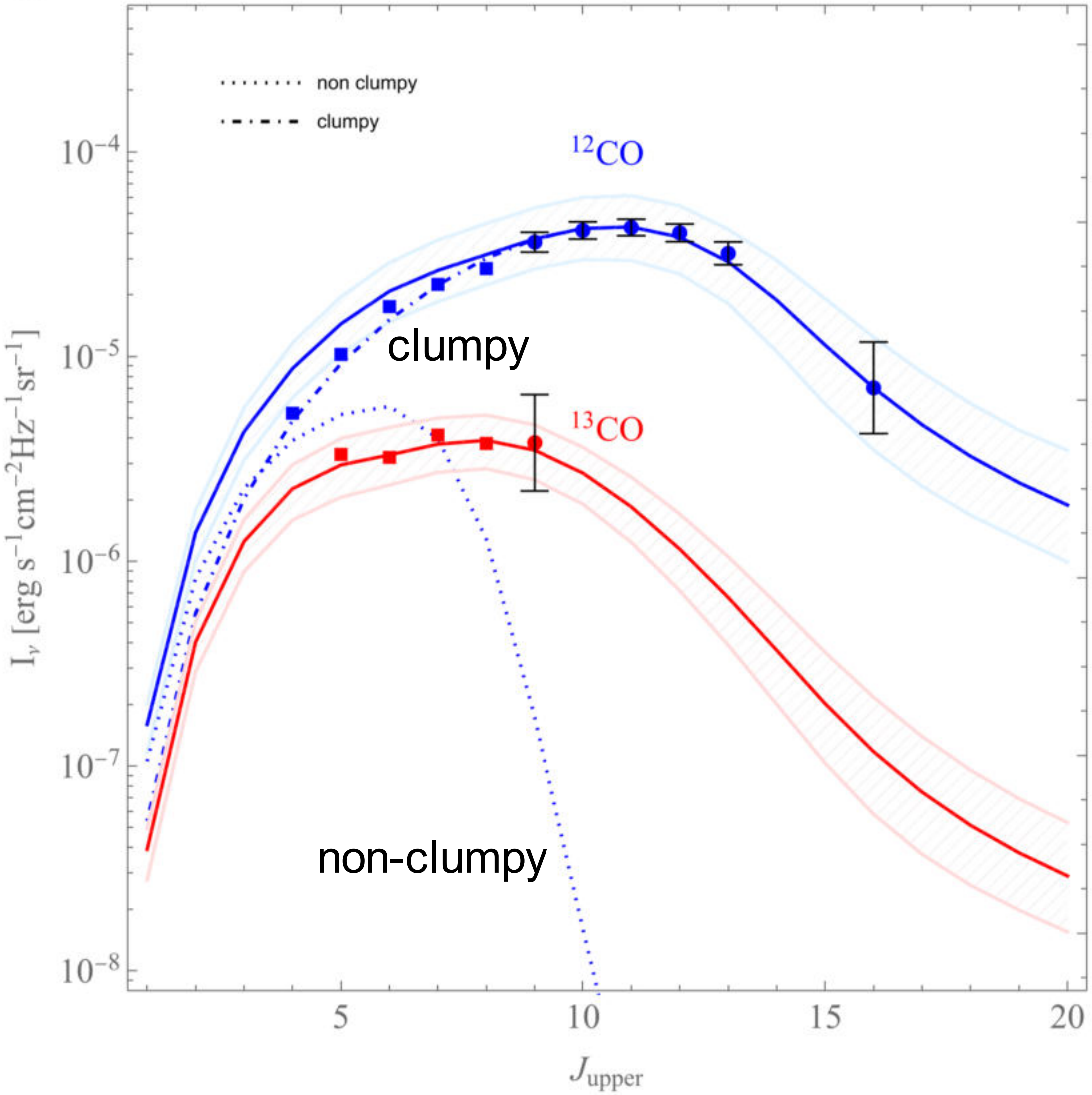

CO-SLED: spectral line energy distribution

2-component model gives best fit

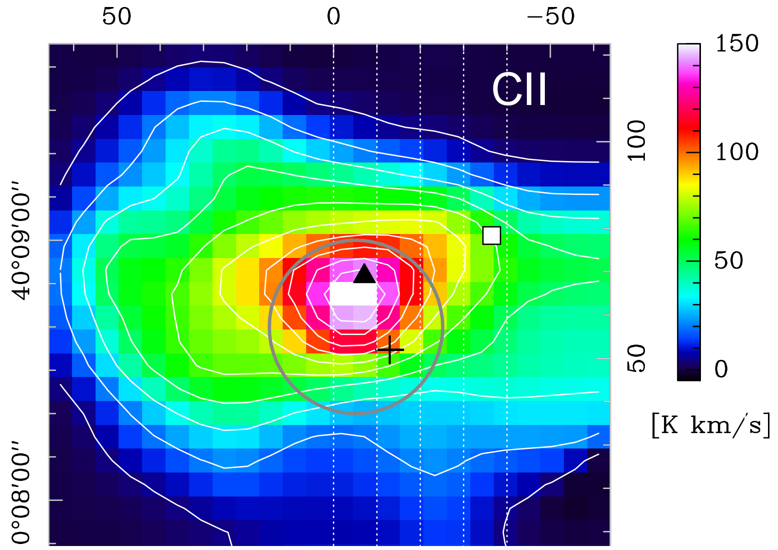

A physical model of the globule   PDR modelling of the head

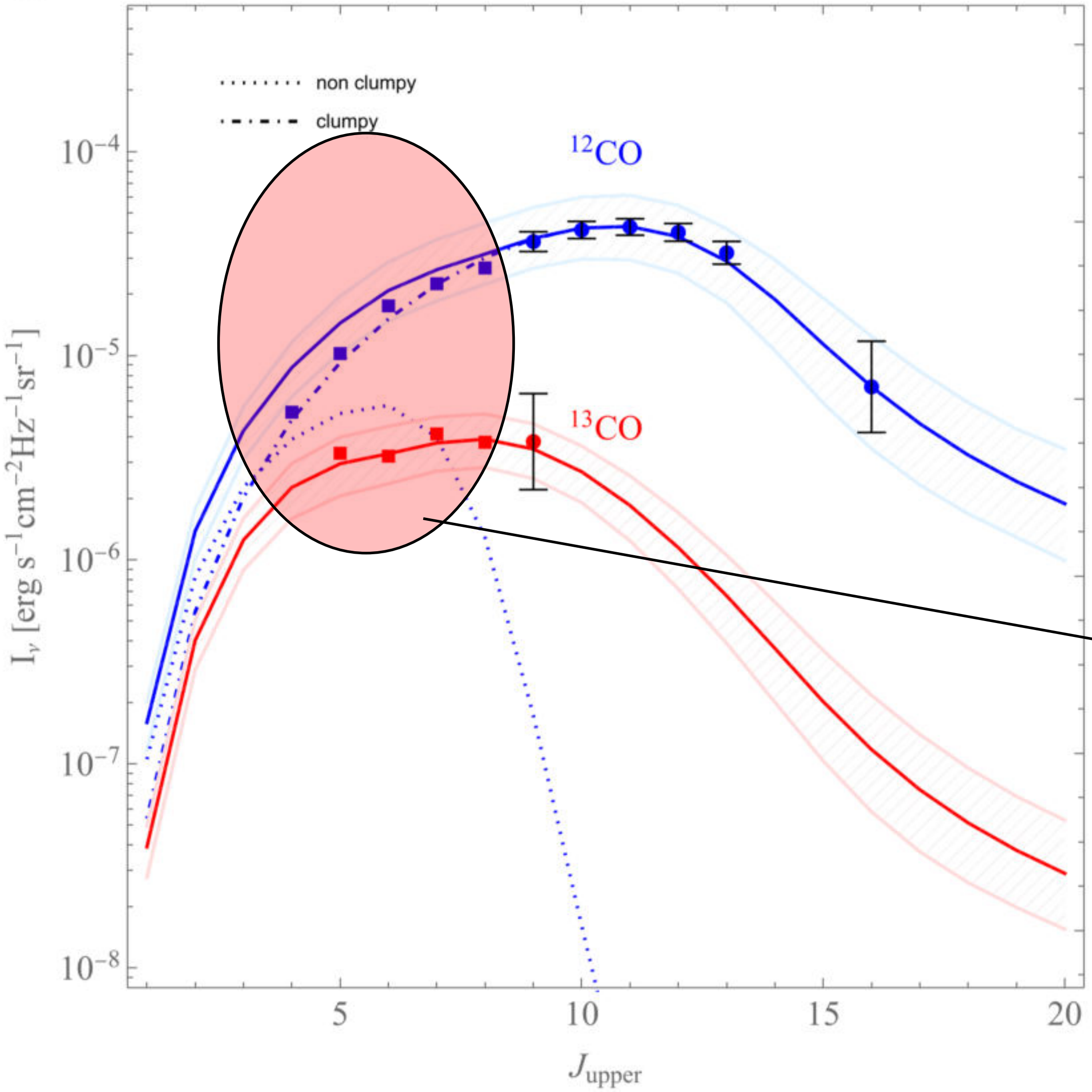

SLW data
excluded in fit

CO-SLED: spectral line energy distribution

2-component model gives best fit

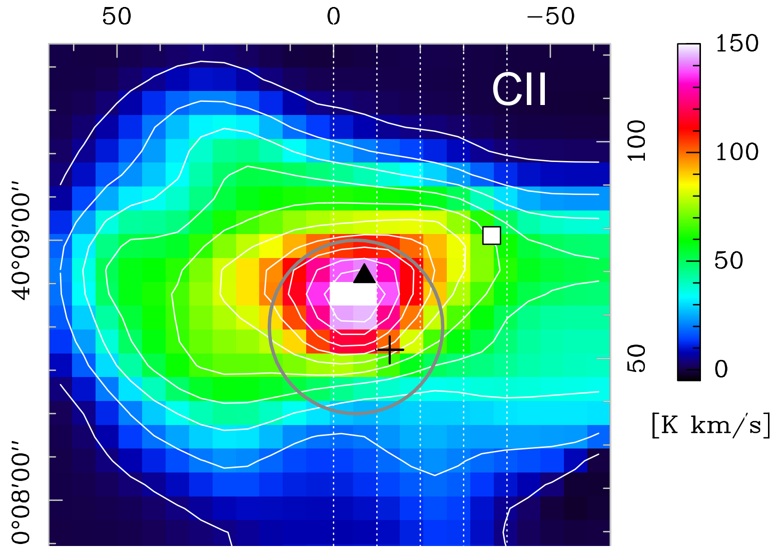

A physical model of the globule PDR modelling of the head

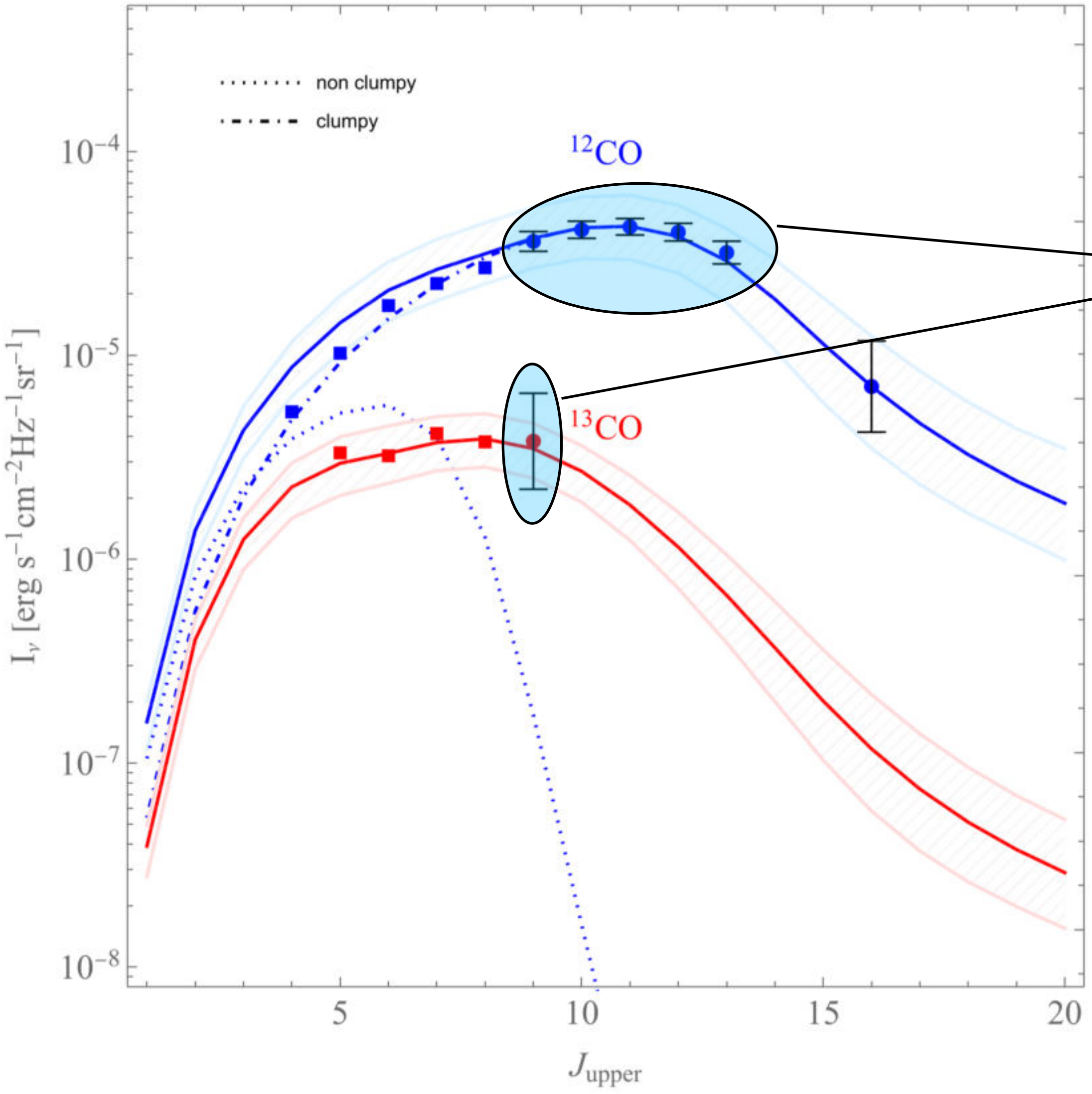

SSW data @ 20‘‘
included in fit

CO-SLED: spectral line energy distribution

2-component model gives best fit

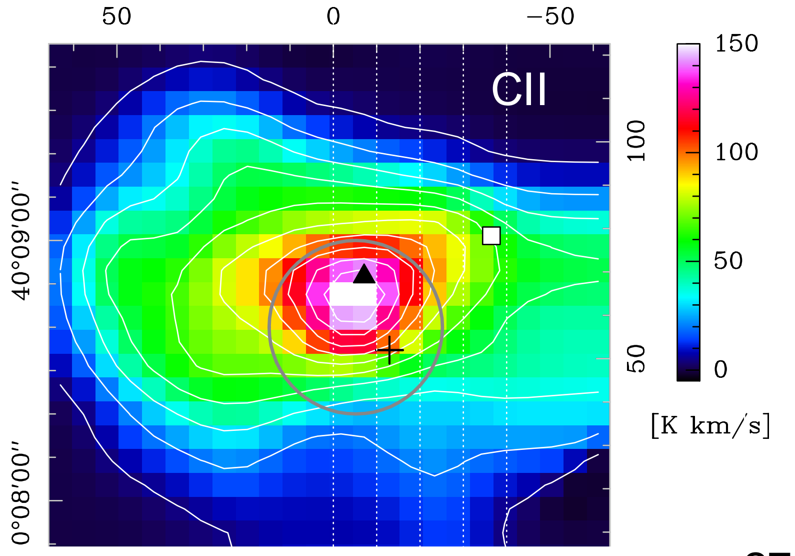

A physical model of the globule

PDR modelling of the head

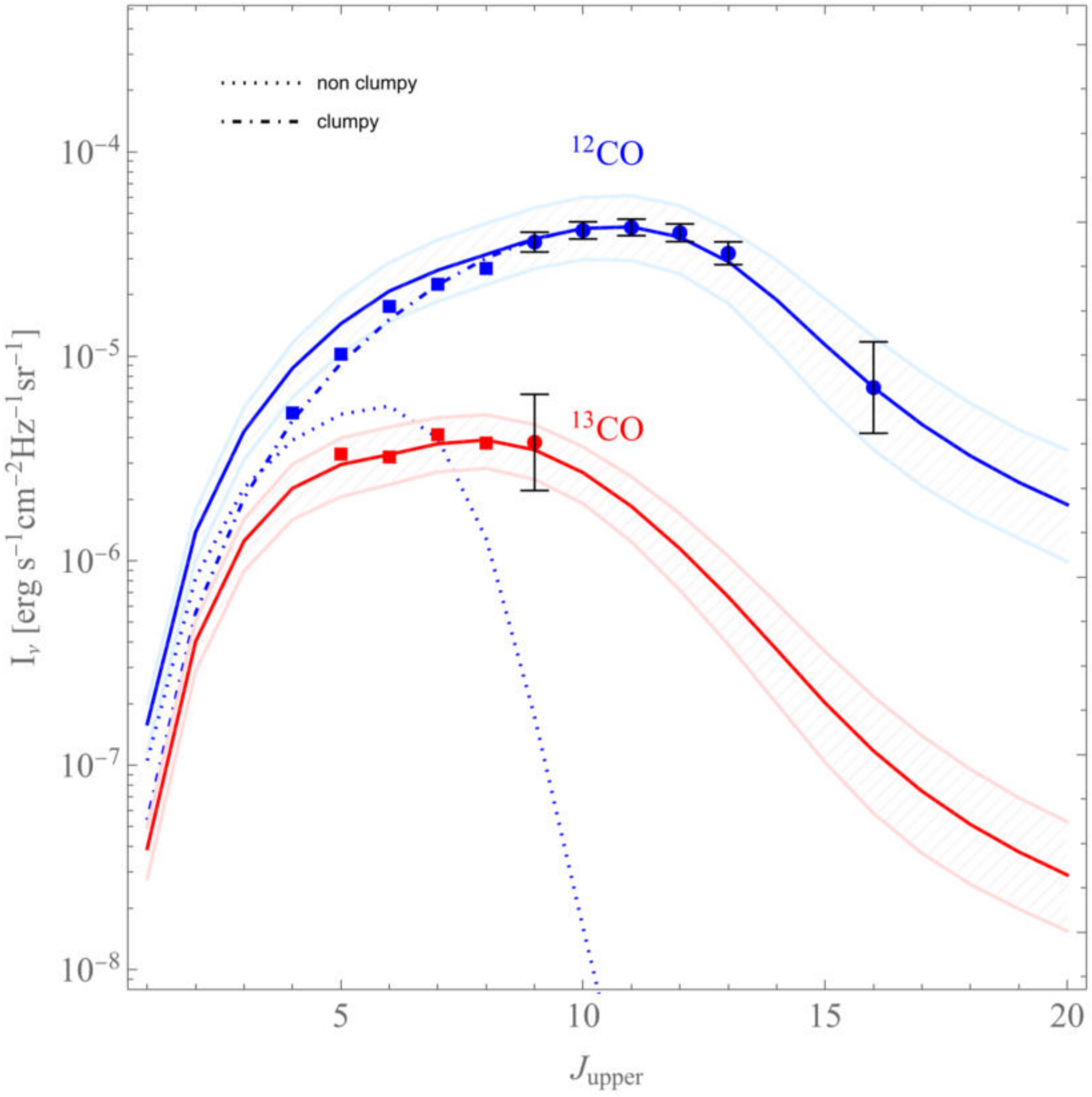

↕ parameter sensitivity

CO-SLED: spectral line energy distribution

2-component model gives best fit

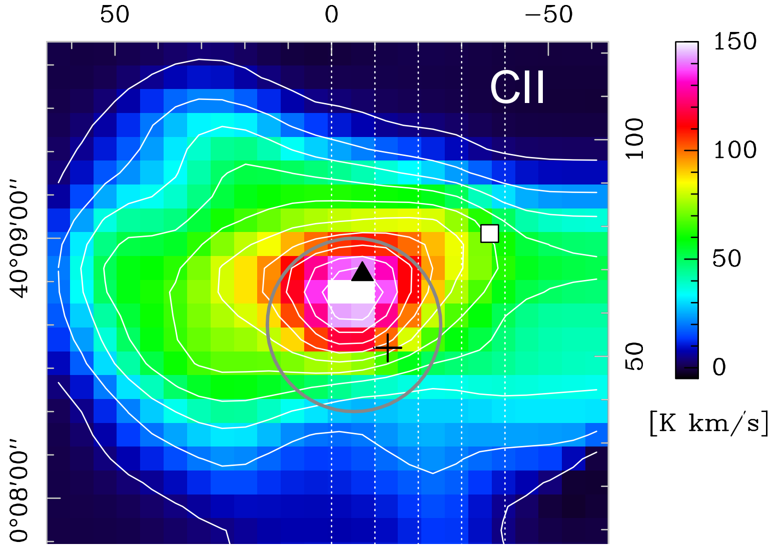

A physical model of the globule

PDR modelling of the head

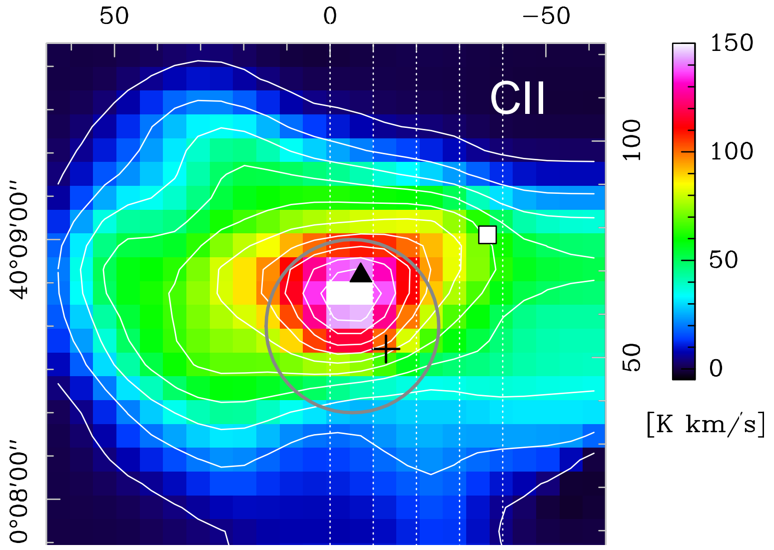

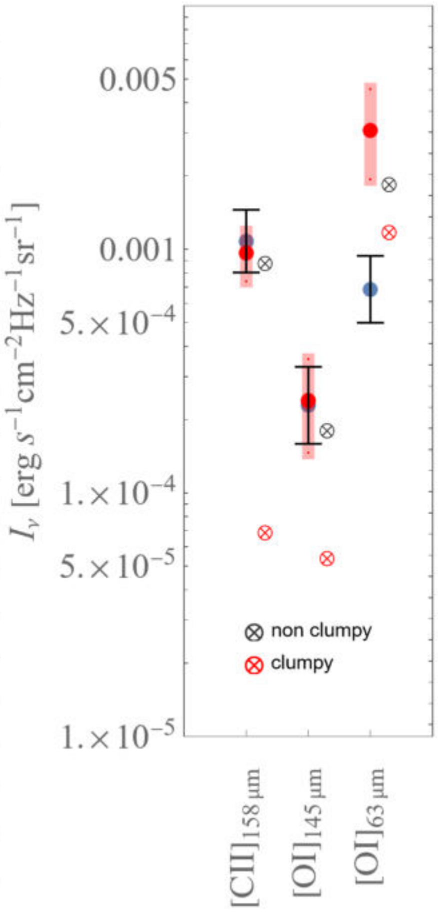

Fine-structure line emission

A physical model of the globule

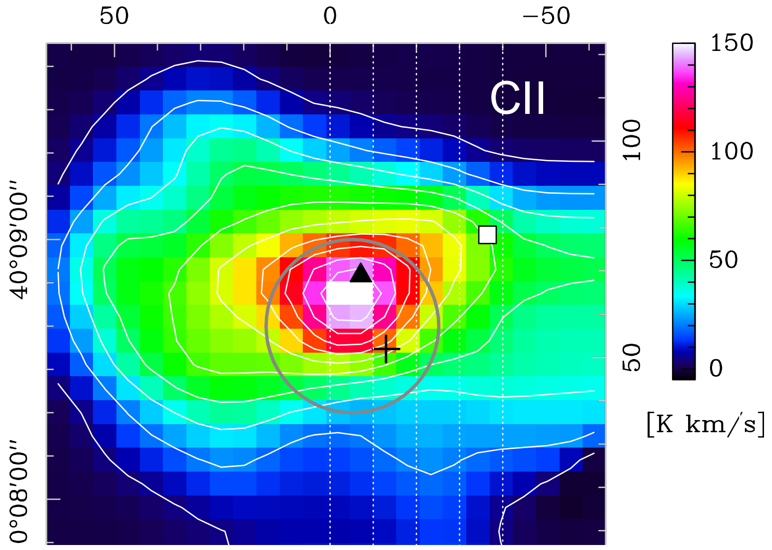

PDR modelling of the head

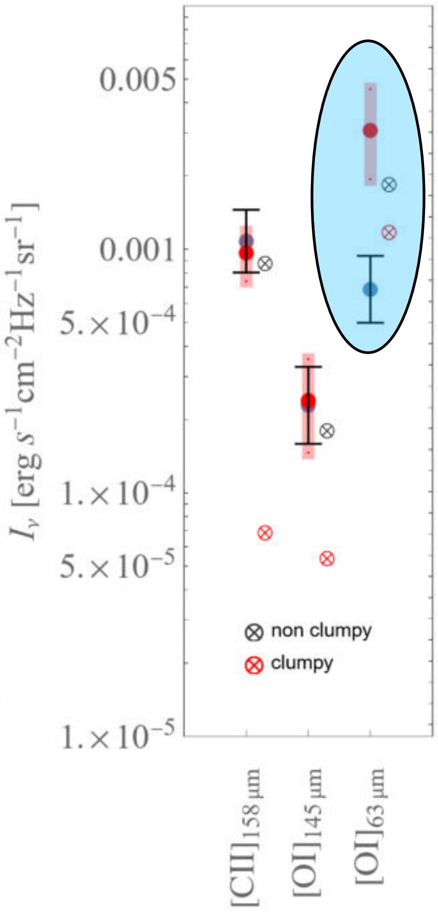

OI 63µm model too strong

→

Explained by foreground absorption.

Observed everywhere

Fine-structure line emission

A physical model of the globule

PDR modelling of the head

[CII] 158 µm & [OI] 145 µm
Fully explained by non-clumpy
EXTERNAL PDR

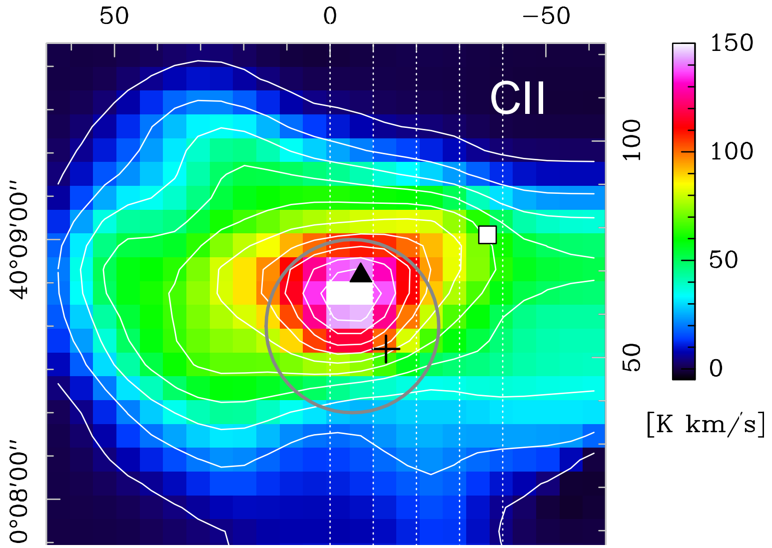

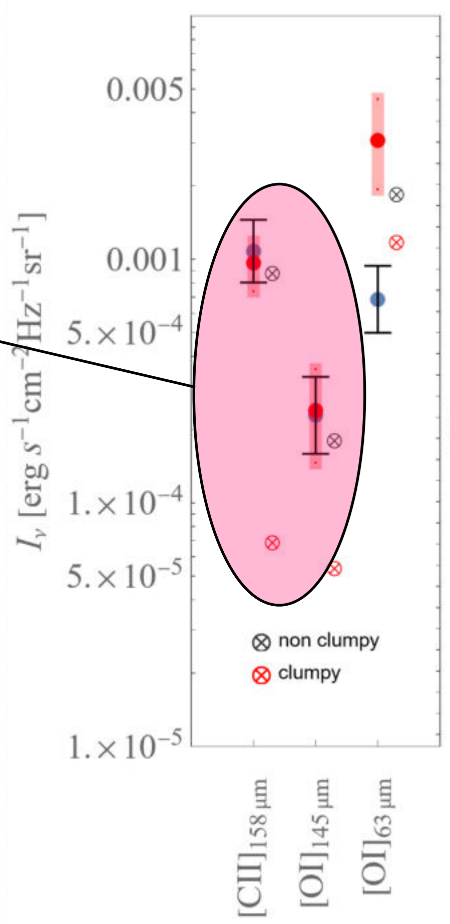

Fine-structure line emission

A physical model of the globule

PDR modelling of the head

Intensity ratios for all lines @ different spatial resolution
Included in fit!

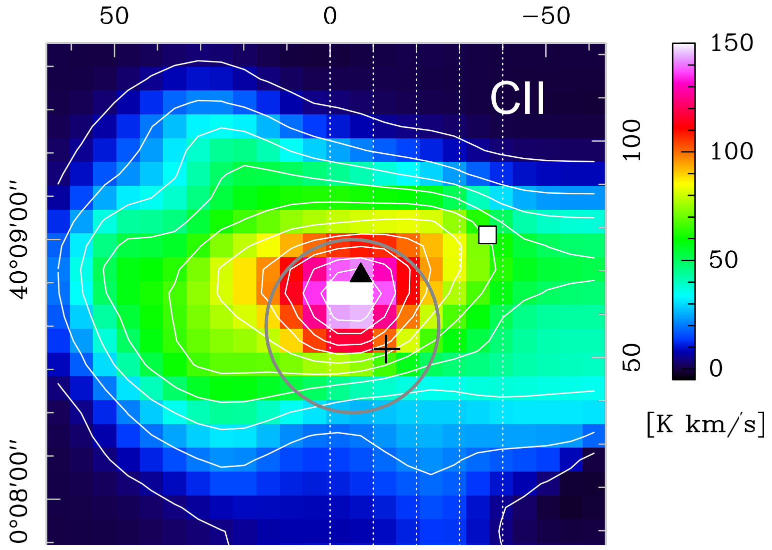

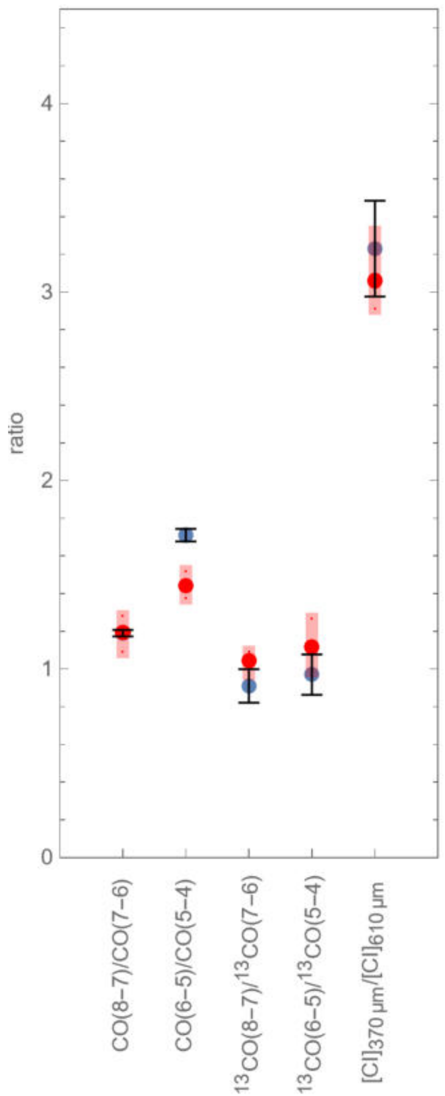

A physical model of the globule PDR modelling of the head

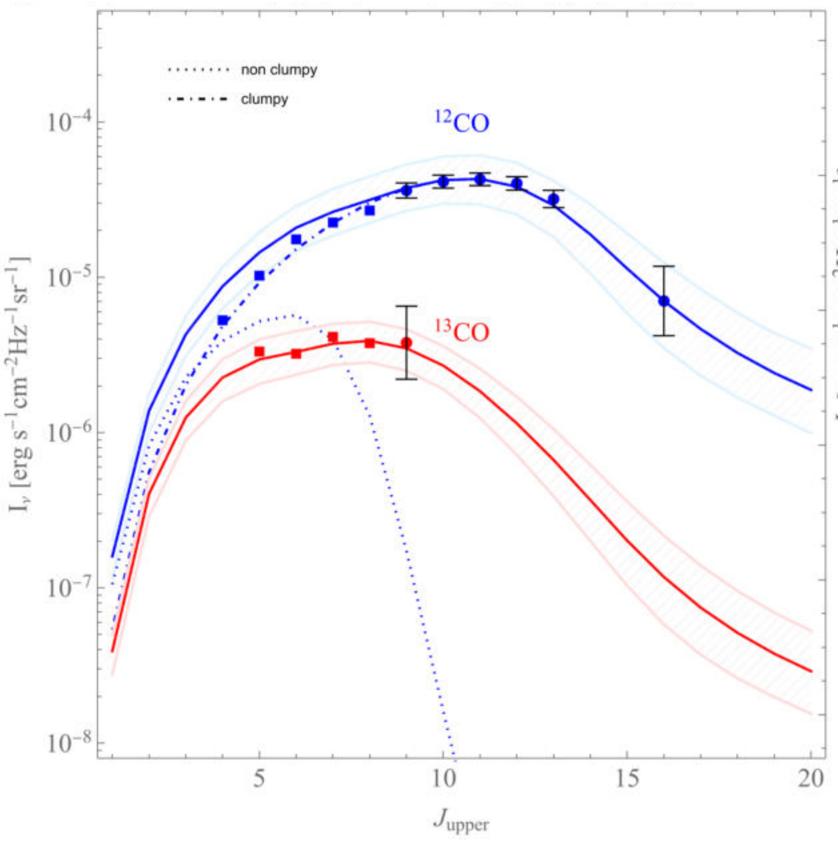

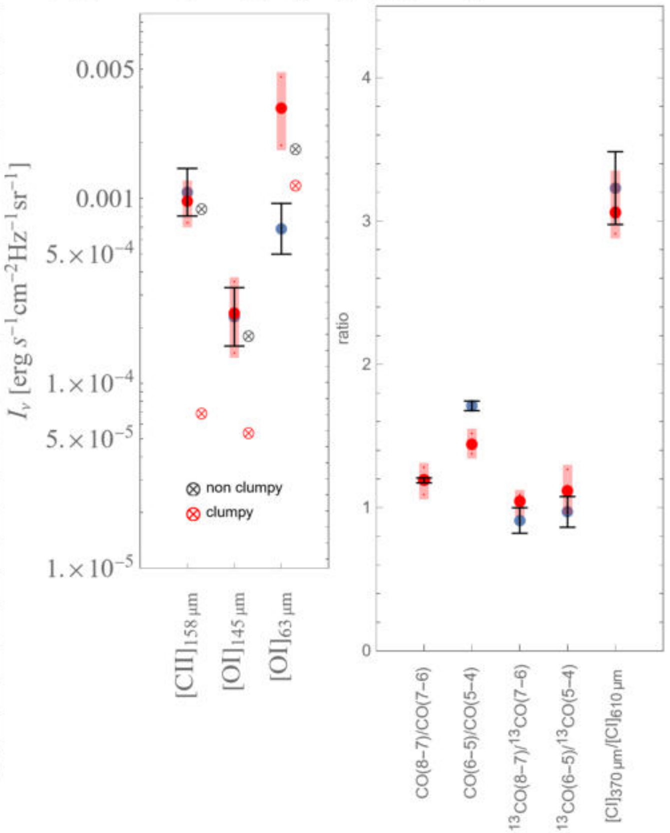

We need the **external** AND the **internal** UV/PDR to explain the emission of the head!

Non-clumpy: mass = 160 M_{sun}, n = 10^4 cm^{-3}, beam-filling = 0.9
Clumpy: mass = 1.1 M_{sun}, n = 1.8 10^6 cm^{-3}

A physical model of the globule

2-component PDR model explains emission

Non-clumpy component
- [CII] 158 µm
- [OI] 63 & 145 µm

Clumpy component
- Mid/high-J CO

A physical model of the globule

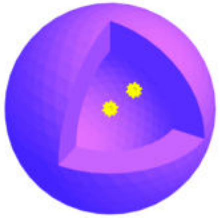

2-component PDR model explains emission

Non-clumpy component
[CII] 158 µm
[OI] 63 & 145 µm

Clumpy component
Mid/high-J CO

HII region

A physical model of the globule

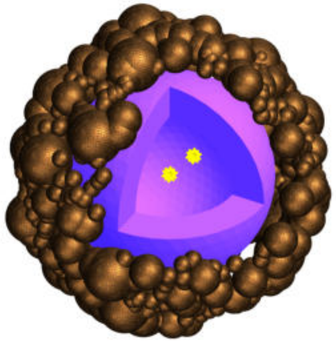

2-component PDR model explains emission

Non-clumpy component
[CII] 158 µm
[OI] 63 & 145 µm

Clumpy component
Mid/high-J CO

+ clumpy
internal PDR

A physical model of the globule

2-component PDR model explains emission

Non-clumpy component
[CII] 158 µm
[OI] 63 & 145 µm

Clumpy component
Mid/high-J CO

+ molecular cloud

A physical model of the globule

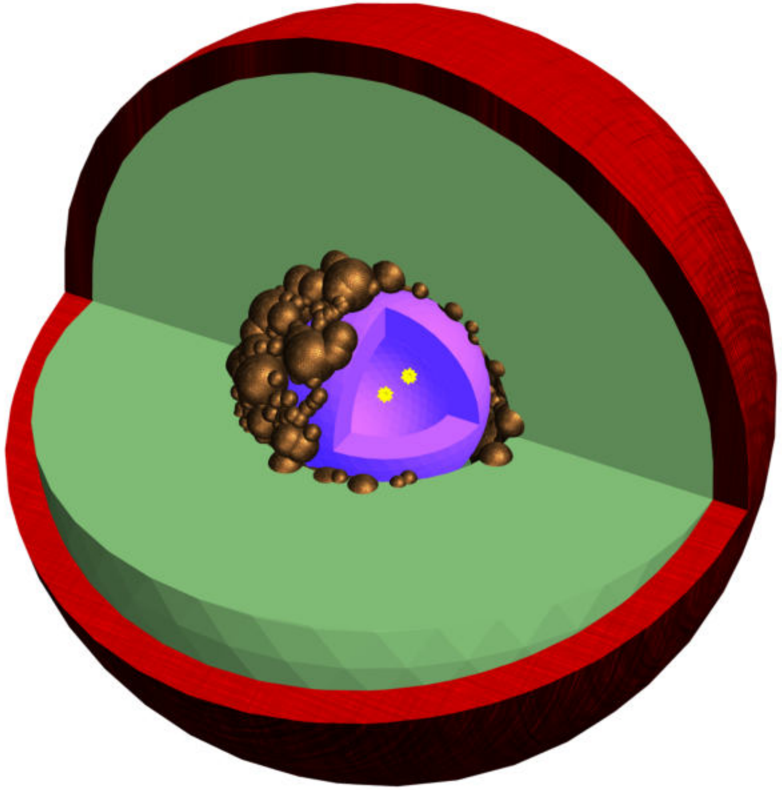

+ external
PDR

2-component PDR model explains emission

Non-clumpy component
[CII] 158 µm
[OI] 63 & 145 µm

Clumpy component
Mid/high-J CO

A physical model of the globule

2-component PDR model explains emission

External PDR: **Illuminated by Cyg OB2**
Non-clumpy component
[CII] 158 µm
[OI] 63 & 145 µm

Internal PDR **Illuminated by internal stars**
Clumpy component
Mid/high-J CO

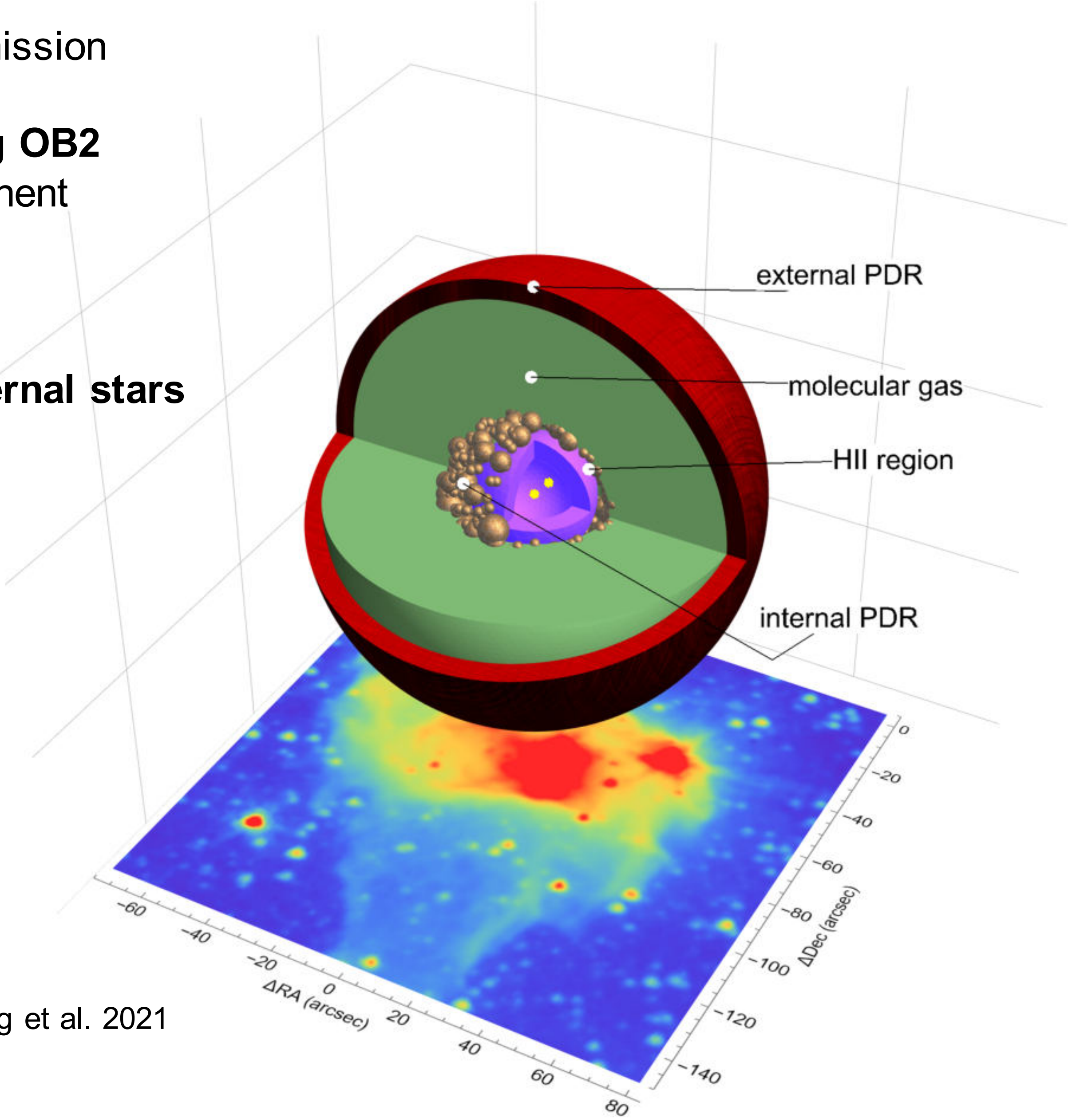

Schneider, Röllig et al. 2021

A physical model of the globule PDR modelling of the tail

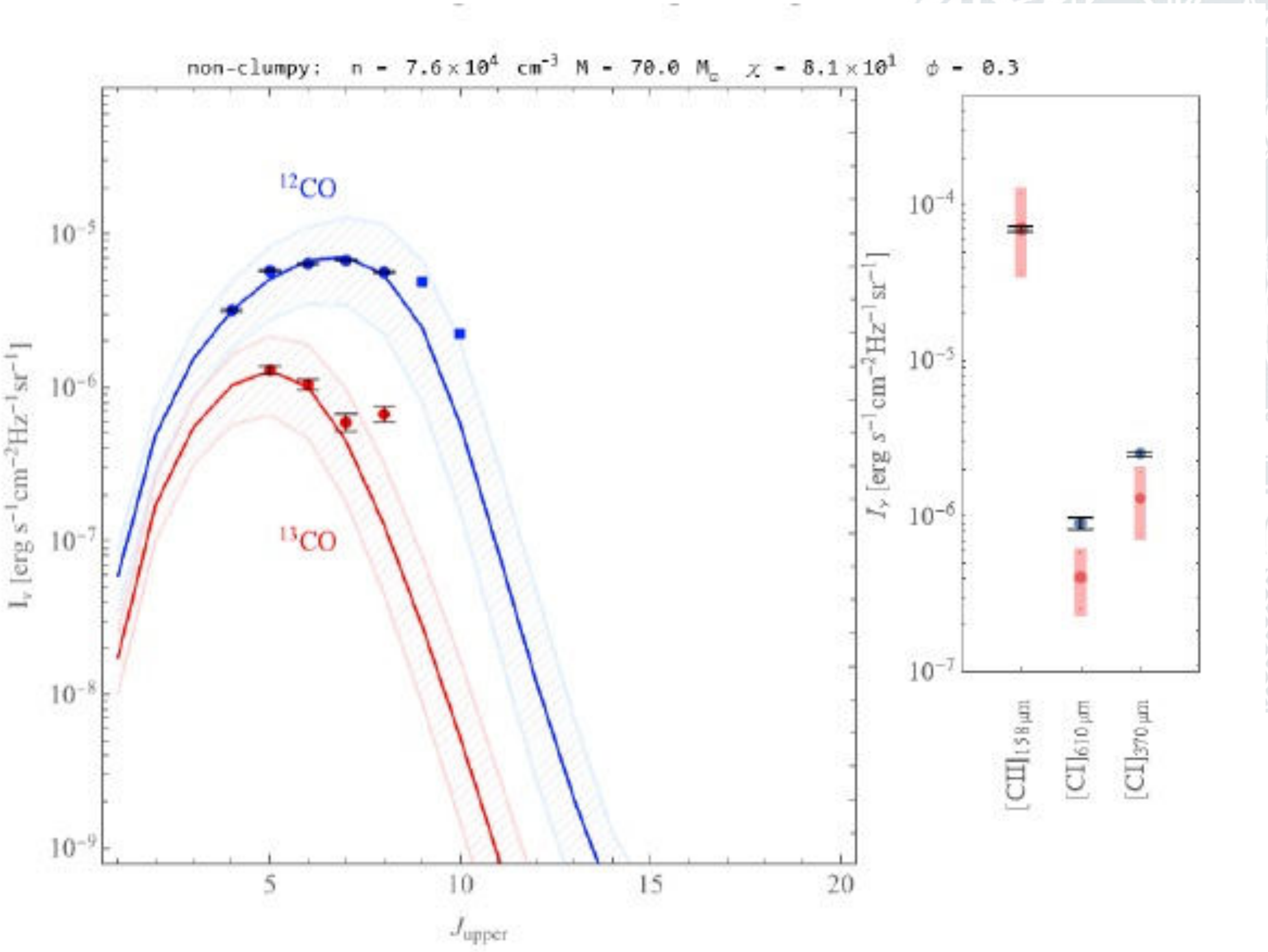

The tail emission can be explained with a **single non-clumpy PDR**.

Summary

- The globule IRAS 20319+3958 is a free-floating globule with a head-tail structure with **embedded high-mass star-formation**, i.e. three star systems with an Herbig Be star and an IR cluster.

- The Herbig Be star is associated with an **outflow in CII**. It is unclear if this is a YSO outflow (star-disk interaction) or dynamics in the HII region/molecular cloud interface.

- The globule shows observational signatures of **rotation**.

- Two positions (one in the head and one in the tail) were observed in a number of PDR cooling lines and modelled with the **KOSMA-tau** model:

  -> The [CII] 158 μm, [OI] 63 and [OI] 145 μm lines can be explained by **external illumination by Cyg OB2** on a non-clumpy PDR.
  -> The mid/high-J CO can be explained by an **internal, clumpy PDR** excited by the massive embedded stars.

Outlook More sources to be studied in FEEDBACK

http://feedback.astro.umd.edu

- **SOFIA legacy program** (PIs N. Schneider, A. Tielens) to map CII at 158 µm and OI at 63 µm using upGREAT in **11 Galactic** star-forming regions.
- **96 h** observing time, observations started in 2019.
- Objective is to study **stellar feedback from massive stars** on the interstellar medium (ISM), i.e. the dynamic evolution of molecular clouds, heating- and cooling processes, and triggering of star-formation.

Visible from Palmdale/New Zealand/both locations

Source	RA(2000)	Dec(2000)	d	V_{lsr}	SF activity	Morphology	Area
	[h m s]	[o ' "]	kpc	km/s	SpT & cluster		arcmin
RCW36	08 59 00	-43 48 49	0.7	5	O8, B-cluster	Bipolar	~15x15
RCW79	13 40 18	-61 44 12	4.3	-50	2 O4, 10 late O	Bubble	~20x20
RCW49	17 12 18	-38 27 43	4.2	0	2WR, 12 early O, compact cluster	Bubble	~20x30
RCW120	17 12 18	-38 27 43	1.3	-10	1 O7	Bubble	~15x15
NGC6334	17 19 03	-35 48 56	1.35	-5	mini starburst	Ridge	~20x35
M17	18 18 31	-16 34 52	1.9	22	2 O4 10 late O	Ridge	~20x30
M16	18 18 56	-13 48 26	2.0	25	O4, 10 late O	Pillars	~20x30
W40	18 30 15	-02 44 31	0.26	5	1 O, 2 B	Bipolar	~20x30
W43	18 46 54	-02 14 11	5.5	100	mini starburst	Ridge	~20x30
Cygnus X	20 37 59	41 45 09	1.4	-3	Nearby Cygnus OB 2: 3 WR,~50 O	Ridge	~20x35
NGC7538	23 13 40	61 30 00	2.8	-55	O3	Bubble	~15x15